CRITICAL REVIEW

Check for updates

Recent advances in nanoparticle-based lateral flow immunoassay as a point-of-care diagnostic tool for infectious agents and diseases

Ruptanu Banerjee [iD] and Amit Jaiswal [iD] *

Lateral flow immunoassay (LFIA) technology is a paper-based, point-of-care strip biosensor designed to detect a specific analyte in a given sample. This type of assay is now of great interest to researchers for its cost-effectiveness, simplicity, portability and rapidness of detection of analytes, including but not limited to areas such as agriculture, food, biomedicine and pathogen detection. Various nanoparticles (such as metal nanoparticles, carbon-based nanoparticles, quantum dots, lanthanides and up-converting phosphor) functionalized by an antibody to detect an analyte protein or molecular marker present in the surface of an infectious pathogen are used for in LFIAs. Herein, we review the principle of the assay and recent advancements made in terms of the different approaches and designs of the assay towards the detection of infectious agents and diseases.

1. Introduction

Lateral flow (immuno) assay (LFIA) is the technology behind many detection devices for the low-cost, fast and simple detection of an analyte of interest in a sample of a complex mixture, where the sample is placed on the test device and the results

School of Basic Sciences, Indian Institute of Technology Mandi, Kamand, Mandi-175005, Himachal Pradesh, India. E-mail: j.amit@iitmandi.ac.in

are displayed within few minutes. Originally, this technique was called the "sol particle immunoassay", as it was first introduced by Leuvering *et al.* in 1980;[1] however, nowadays it is more commonly known as LFIA. In recent years, LFIA-based diagnostic devices have been widely studied because of the low development cost and vast range of applications across multiple areas where rapid detection is a requisite. Another major advantage of LFIA-based tests is that they can be performed on a variety of biological samples, including plasma,[2] sweat,[3,4]

Ruptanu Banerjee received his B.Tech. in Biotechnology in 2016 from the Heritage Institute of Technology, Kolkata, India. He worked as an Indian Academy of Science sponsored summer research fellow at CSIR-NCL, Pune, in 2015 and as a Khorana scholar at the University of Massachusetts Amherst, MA, USA, in 2017. He is currently pursuing his M.Tech. degree in Biotechnology from the Indian Institute of Technology, Mandi,

Ruptanu Banerjee

India. Presently, he is working under the supervision of Dr Amit Jaiswal and his primary research interest is in the applications of nanoparticles for disease diagnosis and as antimicrobial agents.

Amit Jaiswal is presently an assistant professor in the School of Basic Sciences at the Indian Institute of Technology Mandi, India. He completed his PhD in Nanotechnology from the Indian Institute of Technology Guwahati, India, and post-doctoral research from Washington University in St Louis, USA, and Technion – Israel Institute of Technology, Haifa, Israel. His research interest is in the synthesis of nanomaterials for

Amit Jaiswal

sensing, catalysis, drug delivery and diagnostic applications. He has received the Department of Atomic Energy (DAE) Young Scientist Research Award. He is also associated with the BioX centre and Advanced Materials Research Centre at IIT Mandi, India.

saliva,[5,6] serum,[7,8] urine[9,10] and whole blood,[11,12] and the quantity of sample required for detection is much less than that needed with conventional assays.

Since its development, LFIA has achieved penetration in a broad spectrum of markets. Fig. 1 depicts the application in various industries where LFIAs are already in production or are known to be in the development stages.[13] Amongst the different applications of LFIA-based tools, one of the major areas is detecting infectious diseases. Over the year, various detection methods have been implemented for the fast, correct and low-cost detection of infection-causing pathogens or molecular markers associated with them, such as antigens or proteins.[14] LFIA allows a wide range of qualitative, semi-quantitative and quantitative detection of infectious diseases caused by pathogens with high specificity and selectivity.[15] In general, disease diagnosis and its subsequent treatment or prevention heavily depend on highly skilled professionals. LFIA devices can bridge the gap between the production of highly sensitive and selective data for the diagnosis of disease and use by minimally skilled or trained personal to produce results in a very short time.

In a global scenario, nearly 9 million people die annually due to various infectious diseases (tuberculosis, gonorrhoeae, HIV/AIDS, hepatitis, dengue, chikungunya to name a few), which accounted for about 15.8% of all deaths in 2015.[16] The diagnosis of infectious diseases is mostly laboratory based, time consuming (several days to months) and requires well-equipped technical facilities and highly trained technicians. It is clear that for infectious diseases, diagnostics play a valuable and critical role in the care of patients with the disease and for those at risk of developing them. Early diagnosis reduces the chances of death or the severity of the disease as there are various treatments available ranging from vaccination to anti-bacterial drug supplementation. In this scenario, point-of-care (POC) tests, like LFIA, emerge as a key protagonist in fulfilling the necessities of an early test that has a comparable confidence with laboratory-based diagnostic methods and also the advantages of being rapid, simple, low-cost and can be performed irrespective of the need for a laboratory set-up or a trained person for its operation.

The global risk of infectious diseases is very high and in the upcoming years developing countries will face a major threat of pandemics (Fig. 2).[17] Over the past few decades, nanoparticle-based lateral flow biosensors have rapidly been developed to meet the diagnostic needs for detecting infectious diseases. In the present review, we emphasize the detection of infectious diseases with nanoparticle-based LFIA devices. Nanoparticles are used as a probe molecule and serve as the detection module of the LFIA device. Nanoparticles have become a material of choice for probes due to their robustness, size- and shape-dependent tuneable opto-electronic properties, rapid synthesis and ease of functionalization, biocompatibility, persistent stability, capability for visual signal interpretation with a high signal-to-noise ratio and low developmental cost. There are several interesting reviews available covering the fabrication of LFIA devices using various labels and their application towards biosensing.[14,15,18–26] However, only one review, published in 2010 by Ngom *et al.*, covered the application of lateral flow test strip devices for the detection of infectious agents and chemical contaminants.[27] After this, several new strategies as well as improvements were implemented with new-age technology for the detection of biomarkers of infectious diseases. The present review aims to provide a comprehensive collection of all the upgrades and recent trends in the detection of infectious diseases using nanoparticle-based LFIA devices.
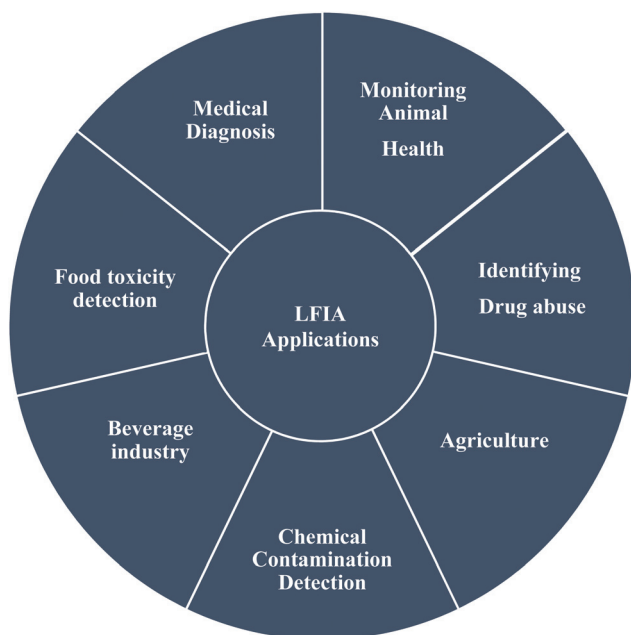
2.   Principle of the assay

The principle behind the lateral flow assay is the movement of the liquid sample or the sample containing the analyte of interest along a strip (Fig. 3). The strip is made with polymeric materials and has specific zones or sites where molecules have been conjugated with a label. When the analyte-containing sample passes through these zones, it interacts with molecules designed to bind specifically to the analyte present in the sample.

As shown in Fig. 3; a sample pad placed at one end of the strip helps to promote and evenly distribute the sample to its next component, the conjugate pad. The sample pad is generally made up of cellulose, cross-linked silica or glass fibres.[15,26] The choice of material to produce a sample pad is based on the material's property to hold certain buffer solutions, proteins, surfactants, *etc.*, while applying the test material to facilitate the flow upon addition of the buffer.[28] The conjugate pad, which is generally made of cross-linked silica, is used to hold the probe particles and keeps them func-

Fig. 1   Markets for LFIA as a POC tool or for on-field technology use.
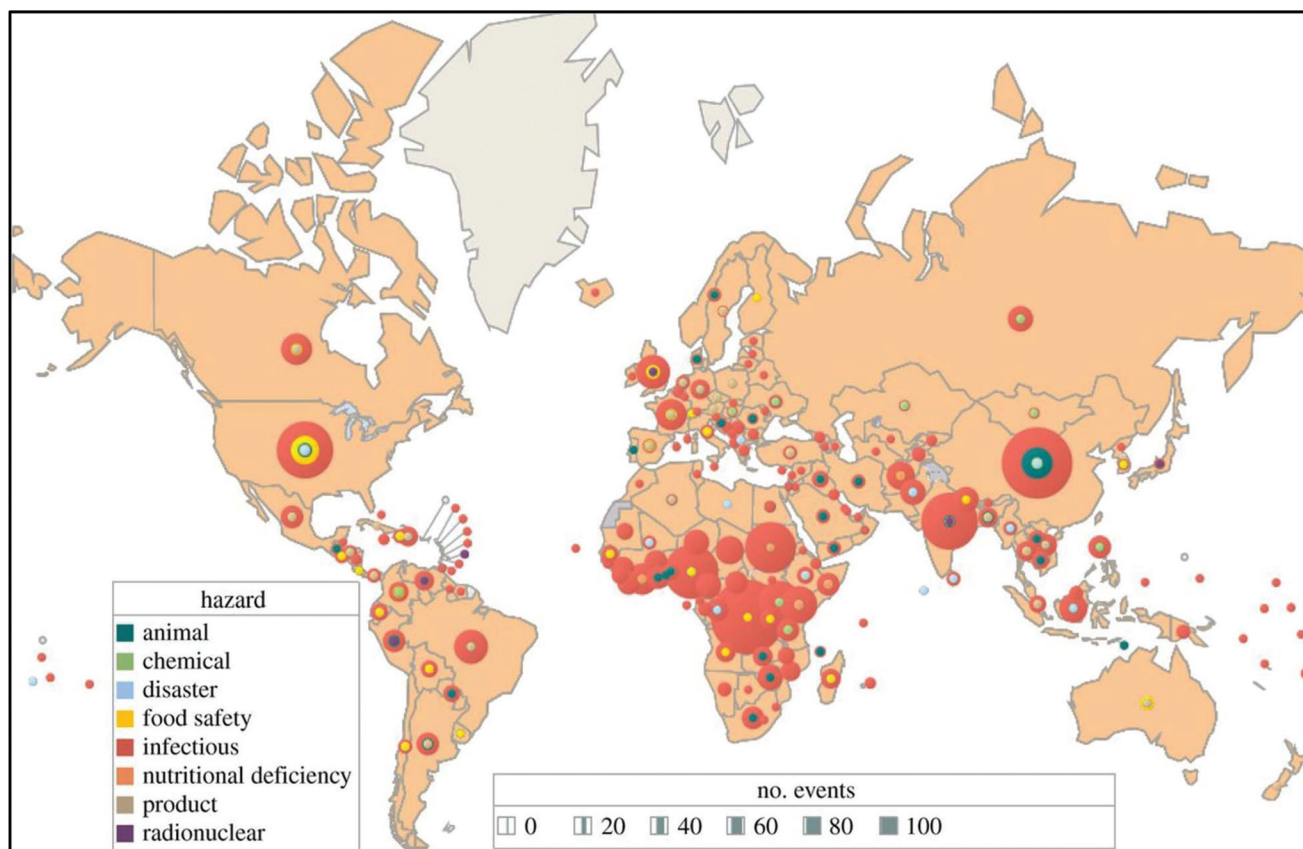
Fig. 2 A total of 2797 international health hazards by type and country, January 2001–September 2013. Eighty-four percent were outbreaks of infectious diseases. Unpublished WHO data (2013). Reprinted (adapted) with permission from ref. 17. Copyright (2014) The Royal Society Publishing.
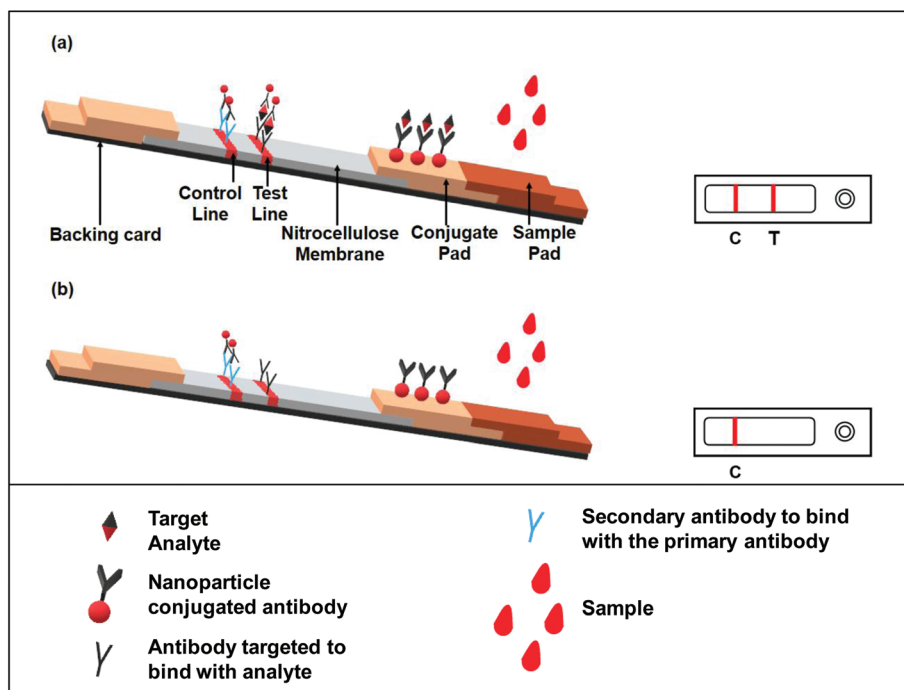

Fig. 3 Schematic representation of a LFIA device; (a) positive result showing the analyte of interest us present in the sample, (b) negative result indicating the analyte of interest is not present in the sample.

tionally stable and active. Additionally, the interaction between the nanoparticles and the sample pad should be weak in order to release the conjugated particle when encountering a moving fluid. This is accomplished by using a buffer or mixture of buffers typically containing carbohydrate molecules. These sugar molecules (like sucrose) stabilize the probe particles by forming a layer around them, thus shielding the particles from degradation.[29] The probe particles are conjugated to an antibody or a molecule that specifically binds to the target analyte. In most cases, the probe used is a conjugated colloidal gold nanoparticle (AuNP). However, a few recent reports have also demonstrated the use of other nanoparticles, like silver,[30] carbon,[31] selenium[32] or coloured latex particles,[33] as a probe for LFIA devices. After crossing the conjugate pad, the flowing fluid, now also carrying the probe particles either free or bound to the target analyte (if present in the sample), comes into a membrane typically made of nitrocellulose. This membrane has two different zones or lines, namely the test and control zones or lines. Biological components, mainly antigens or antibodies, are immobilized to form these lines. The next step is the interaction between the target analyte and specific antibody coated in the test and control zones. The design of the assay is made in such a way that if the analyte of interest is present in the sample, it will be captured by the antibody present in the test zone. This antigen–antibody aggregation will result in developing a colour or band formation at the site of the test zone depending upon the type of label used (such as AuNPs).[34] To conclude that the flow through the membrane has been properly established, the response in the control zone is observed. This is independent of the target analyte and it will always form the band even if there are no analyte molecules present in the given sample. This happens because of the interaction of the unloaded probe and the antibodies present in the control zone. A positive test is indicated by the development of bands at both the test and control regions, while band formation only in the control zone demonstrates a negative test (Fig. 3). A response either only in the test zone but not in the control zone or no response at all in any of the zones is indicative of an invalid result.[21]

There are two types of format exploited for the immunoassay: sandwich and competitive assays.[18] The sandwich format is applicable for analytes with more than one epitope. In this case, one site of the target analyte binds with the antibody conjugated with the label molecule for *e.g.* AuNPs. This antibody–gold conjugated target analyte then flows through the membrane and comes into contact with another antibody specific to any other binding site of the target analyte in the test zone. The capture of the antibody–AuNP–antigen conjugate and antibody present in the test zone makes a pattern or line that can be visually verified or can be detected *via* optical/magnetic detectors based on the type of label used.

When the analyte is of low molecular weight and/or is a hapten, *i.e.* it has only one binding site or epitope, the competitive format is used. In this format, the signal is negatively correlated with the concentration of the analyte.[35] The immobilized analyte conjugated with the antibody–AuNP complex is sprayed over the test line giving a strong response signal. When the analyte flows through the strip, it competitively binds with the antibody and thus releases the antibody–gold nanoparticle conjugate from the test line, and thus the signal gets reduced with increasing the concentration of the analyte.

Nanoparticles are widely used as label or probe molecules for detection in LFIA devices. Coloured or fluorescent nanoparticles in the range of 15–800 nm are ideal as their small size does not interfere with the flow or the path of the flow. As mentioned earlier, though AuNPs are a popular choice for the label, other nanoparticles have also been employed. Liposomes incorporated with bioluminescent dyes,[36] quantum dots,[37] up-converting phosphorus technology[38] and surface-enhanced Raman scattering (SERS) reporters[39–43] are some of the new approaches for achieving better sensitivity and quantitative analysis.

Surface functionalization is a key part of using nanoparticles as a label in LFIA systems. The major role of nanoparticles involved in the sensing of specific analytes in the LFIA platform is their ability to bind with biomolecules, such as antibodies. This conjugation is achieved by adsorption of the ligand moiety onto the surface of the nanoparticle. Though only weak interaction forces are involved in the conjugation process, this can degrade the antibody or the protein attached to it.[44] Hence, the surface functionalization of nanoparticles is done prior to conjugation for stability of the conjugated system. Poly(ethylene glycol) (PEG) is the most commonly used polymer to coat the surface of nanoparticles. PEG modified with a thiol group (–SH) in one end, carboxyl group (–COOH) or amine group (–NH$_2$) in another end is predominantly used as it can attach with the AuNPs surface *via* a thiol bridge and the antibody can attach at the other end *via* an aldehyde-carboxyl/amine interaction.[44] Surface modification with carbohydrate molecules can also be done for potential biosensor and diagnosis applications.[45] For a detailed overview on the surface functionalization of different nanoparticles, readers may refer to ref. 46–49, as this is beyond the scope of the present review.[46–49]

Another form of LFIA is the nucleic acid lateral flow immuno assay (NALFIA), which is used to detect the presence or absence of amplified ds-nucleic acid structure (amplicons) specific to the pathogenic organism. There are several formats reported for NALFIA: (1) ds-amplicon marked with two different tags at two strands, where one is biotin labelled and the other is a fluorescent tag. The avidin-coated nanoparticle binds to the biotin-labelled strand and the anti-tag antibody captures the other strand labelled with the tag and thus the signal produced is directly proportional to the amount of ds-amplicon present.[50] (2) Nanoparticle-conjugated reporter probe and biotin-tagged capture probe for ss-amplicon detection. The capture probe is immobilized by avidin interaction and the amplicon binds with the probe to generate the signal.[51] The capture probe can also be BSA tagged or can be simply immobilized in the strip through passive adsorption.

3. LFIA application strategies for diagnosing infectious diseases

In the following sections, we have divided the LFIA devices into three broad categories based on the type of the disease: 1. pathogenic bacterial strains and toxins and 2. protozoal and 3. viral infections. AuNP is the most exploited nanoparticle reporter in the LFIA devices due to its stability, ease-of-synthesis, surface modification and functionalization for desired change in the physical and chemical properties, which leads to its optimum function as a reporter molecule as needed for the device. Besides AuNPs, carbon nanoparticles (CNPs), quantum dots (QDs), up-converting phosphor (UCP) and other nanomaterials are also being used for the detection of infectious agents through LFIA. A brief discussion on all the above categories is represented in Tables 1 and 2 with a focus on the reported works with promising results along with some enhancement or modification over the existing techniques for improved sensitivity and detection limits.

3.1. LFIA for detecting bacteria and bacterial infections

There are various bacterial toxins and food-borne infectious diseases where LFIA devices are used for rapid detection. Staphylococcal enterotoxin B (SEB) has been reported to be detected using 25 nm colloidal gold as a label with anti-SEB IgG, with a detection limit of 1 ng mL^{-1} in less than 5 minutes.[61] An improvement over conventional SEB detection was reported by using fluorescent immunoliposomes, which allowed the detection of SEB close to 20 pg mL^{-1}.[78] SERS-based enhancement for the detection of SEB has shown a detection limit of 0.001 ng mL^{-1}. Here, MGITC, a SERS reporter conjugated with gold nanospheres, was used as a label in the assay.[40] Anthrax, a deadly infectious disease caused by *Bacillus anthracis*, has also been investigated through LFIA. Anthrax incidents in 2001 and its potential to be used as a weapon in bioterrorism led researchers to develop a method for the fast and sensitive detection of spores causing anthrax in food and feeds.[101,102] For this, an additional step of IMS was performed prior to subjecting the sample to a LFIA device. This proved successful in sensing the spores of *Bacillus anthracis* in water and dairy products with a spore recovery of 95% from IMS[62] with 10^5–10^7 CFU mL^{-1} of spores in the milk or water sample. IMS was achieved by using anti-spore antibodies conjugated with COOH-magnetic beads. A magnet was used to separate the complex, and formamide and EDTA were used to elute the spores, which were then used in the LFIA device (Fig. 4).

Human salmonellosis diagnosis has also been established by LFIA, which was designed to detect *Salmonella enteritidis* with a detection limit of 10^7 CFU mL^{-1} without any cross-reactivity with *Salmonella typhimurium*.[58] As low as 10 CFU mL^{-1} of *Salmonella enteritidis* was detected by using aptamer-based strand-displacement amplification (SDA).[59] In this process, the bacteria were first mixed with an excess amount of aptamers of two types that specifically bind to the bacteria: one of which

is biotin labelled, while the other carries the sequence for SDA. Then, the streptavidin-labelled magnetic beads were used for magnetically separating the *S. enteritidis* bacterium from other species. These magnetic-bead–aptamer–bacteria complexes were then directly amplified by SDA, and the amplified product containing ssDNA was applied on a LFIA test strip and subsequently detected, as shown in Fig. 5. A Gram negative bacterial strain, *Escherichia coli* O157:H7, causes haemorrhagic colitis and hemolytic uremic syndrome in humans.[103] A LFIA strip for the rapid detection of *E. coli* O157:H7 was developed by Jung *et al.* in 2005. This assay was based on murine mAb to the said antigen (*E. coli* O157:H7 LPS) conjugated with 40 nm colloidal AuNPs with a lowest detection limit of 1.8×10^5 CFU mL^{-1} without any enrichment.[52] A later study reproduced a similar detection limit, namely 1×10^5 CFU mL^{-1}, in various food samples, namely milk powder, flour, *etc.*[53] The immunomagnetic enrichment technique further increased the sensitivity for the detection of *E. coli* O157:H7 with a detection limit of 10^3 CFU mL^{-1} with 95.5% sensitivity and 100% specificity.[54] Another study reported aptamer-mediated magnetic enrichment as well as a strand-displacement amplification method for the detection of *E. coli* 0157:H7 with a detection limit of 10 CFU mL^{-1}.[104] In this study, they used two different aptamers that selectively bind to two different outer membrane proteins of *E. coli*. One of the aptamers were biotin labelled and were magnetically enriched by streptavidin-labelled magnetic beads separation. The other aptamer was used for amplification and subsequently targeted for detection *via* NALFIA. In this context, carbon-based nanoparticles and nanomaterials have also been exploited as labels in LFIA devices. Carbon-based nanoparticles are preferred for their very low production cost, high contrast signal and ease of scale-up reactions.[19] The fluorescence quenching of QDs by GO 2D nanosheets as a mechanism for detection has been used to detect as low as 100 CFU mL^{-1} of *E. coli* in bottled water and milk samples.[57] The detection mechanism is described in Fig. 6. When the analyte is not present in the sample, GO can effectively quench the fluorescence of the QDs (OFF mode). In the presence of the target analyte, this quenching is hindered and the fluorescence signal is detected (ON mode). The detection of EPEC and EHEC by using AuNP-based LFIA was also reported with a specificity and sensitivity of 100% and 96.9%, respectively.[65] In-solution hybridization for the detection of specific sequences of 16S ribosomal RNA allowed the detection of 5×10^4 CFU mL^{-1} of *E. coli* within 25 minutes (Fig. 7).[105] *Campylobacter* species are reported as the causative agent for human bacterial gastroenteritis in many industrialized countries.[106] A 15 kDa cell surface protein of *Campylobacter jejuni* has been targeted for the rapid detection by LFIA from human faecal extract. Within 15 minutes, a specificity of 100% and a sensitivity of 84.8% was achieved with the designed LFIA device.[66]

There are various enterobacteriaceae family members (like *Shigella* sp. and *Aeromonas* sp.), for which their detection carried out by LFIA devices. The detailed description of these LFIA device can be found in ref. 107. Enterobacteriaceae

Table 1 LFIA devices for detecting bacterial infection

Bacterial analyte	Sample used for detection	Type of label	LFIA principle	Sensitivity or LOD	Ref.
Escherichia coli O157	Faecal samples from bovine and swine, raw beef, pork	AuNPs	40 nm AuNP-conjugated Murine monoclonal antibody (mAb) to E. coli O157:H7 lipopolysaccharide (LPS)	1.8×10^5 CFU mL^{-1} without enrichment and 1.8 CFU mL^{-1} after enrichment Specificity: pork (98.8%), bovine faeces (87.9%) and swine faeces (93.4%)	52
Escherichia coli O157:H7	Milk powder, flour, starch, coffee, biscuit, cake, jelly and juice	AuNPs	Colloidal-gold-conjugated double antibody sandwich assay	1×10^5 CFU mL^{-1} with no cross-reaction with 30 strains of 24 species in Enterobacteriaceae (including non-O157 E. coli, Salmonella, Shigella, Proteus, Citrobacter, Enterobacter, Serratia and Yersinia), Staphylococus, Listeria, Aeromonas and Vibrios	53
	Spiked milk, purified water and beef	AuNPs	Colloidal gold conjugated with E. coli O157:H7 mAbs. Immunomagnetic separation (IMS) is done by immunomagnetic particle (IMP) conjugated with E. coli O157:H7 polyclonal antibodies (pAb)	Without IMP 10^5 CFU ml^{-1} With IMP 10^3 CFU ml^{-1} Sensitivity: 95.5%	54
Escherichia coli O157:H7	Culture broth	Fluorescent microsphere	Fluorescein isothiocyanate fluorescent microspheres conjugated with E. coli O157:H7 mAbs	1.6×10^3 CFU mL^{-1}	55
Escherichia coli O157 Salmonella typhimurium	Culture broth	AuNPs	AuNP conjugated with antibodies against E. coli O157 and S. typhimurium	E. coli O157: 10^5 CFU mL^{-1} S. typhimurium: 10^6 CFU mL^{-1}	56
Escherichia coli	Standard buffer, bottled water and milk samples	Streptavidin-QD 655 (quenching by Graphene oxide (GO) in absence of pathogen (OFF state))	Streptavidin-QD conjugated biotinylated antibody against E. coli followed by treatment with GO	10 CFU mL^{-1} in standard buffer 100 CFU mL^{-1} in bottled water and milk	57
Salmonella enteritidis	Raw eggs	AuNPs	Anti-S. enteritidis antibodies conjugated to colloidal gold particles	10^7 CFU mL^{-1} No cross-reactivity with Salmonella typhimurium	58
	Bacteria spiked milk powder	AuNPs	15 nm AuNP-conjugated DNA	10 CFU mL^{-1}	59
	Simulated samples of human urine, serum and cow milk powder	AuNPs	AuNP-conjugated 16s rDNA/rRNA	5 fmol for synthetic DNA	60
Staphylococcal Enterotoxin B		AuNPs	25 nm AuNP conjugated with purified anti-SEB IgG	1 ng mL^{-1} With silver enrichment: 10 pg mL^{-1}	61
Anthrax (Bacillus anthracis)	Milk, water samples	AuNPs	IMS of anthrax spores followed by lateral flow assay with AuNP as label	5×10^5 CFU mL^{-1}	62
Bacillus anthracis	Culture media	Super-paramagnetic nanoparticles	mAb 12F6 conjugated to super-paramagnetic iron oxide particles	400 pure B. anthracis spores 4×10^3–10^6 CFU mL^{-1}	63
Bacillus anthracis	Spiked samples of milk powder, starch and baking soda	Carboxylated super-paramagnetic iron oxide particles	mAbs 12F6 against B. anthracis conjugated with super-paramagnetic iron oxide particles	500–700 pure B. anthracis spores 6×10^4 spores per g in milk powder, 2×10^5 spores per g in starch and 5×10^5 spores per g in baking soda	64
Enteropathogenic E. coli (EPEC) and enterohemorrhagic E. coli (EHEC)	Supplemented stool sample	AuNPs	AuNP-conjugated anti-EspB IgG	4 ng mL^{-1} In stool sample: 0.06 µg mL^{-1} Sensitivity: 96.9%	65
Campylobacter jejuni	Faecal extract	AuNPs	mAb (4B4) against a 15 kDa cell surface antigen-colloidal gold conjugate	1.8×10^4 to 8.2×10^4 CFU mL^{-1} Sensitivity – 84.8%	66
Aflatoxin B1 (AFB1)	Culture media	GO or carboxylated GO (GO-COOH)	Anti-AFB1 mAb labelled with GO or GO-COOH	Visual LOD: 0.3 ng mL^{-1}	67
Aflatoxin B$_2$ (AFB$_2$)	Culture media	Magnetic nanogold microspheres with nano-Fe$_2$O$_3$ particles as core and AuNPs as shell	Monoclonal anti-AFB2 antibody (clone 3A7) conjugated Nano-Fe$_2$O$_3$ particles	27 µg kg^{-1}	68

Table 1 (Contd.)

Bacterial analyte	Sample used for detection	Type of label	LFIA principle	Sensitivity or LOD	Ref.
Aflatoxin M1 (AFM1)	Spiked raw milk	Immuno magnetic nanobeads (MNB)	MNBs conjugated with anti-AFM1 antibody	0.1 ng ml^{-1} in raw milk	69
Aflatoxin M1 (AFM1)	Raw milk samples	Immuno MNB	Anti-AFM1 mAb conjugated MNBs	0.02 µg L^{-1}	70
Fumonisin mycotoxins	Maize flour sample	CdSe/ZnS QDs	BSA tagged fumonisin antigen conjugated with QD (fluorescence quenching by AuNP-conjugated anti-fumonisin antibody)	Visual LOD: 1.56–6.25 ng ml^{-1}	71
Botulinum (*Clostridium botulinum*)	Spiked faecal sample	AuNPs	AuNP-conjugated monoclonal Botulinum Neurotoxin Type D (BoNT/D) antibody	50 pg ml^{-1}	72
	Spiked samples of serum, urine and cooked meat broth	AuNPs	AuNP-conjugated anti-BoNT/A heavy chain mAb (44.1)	50 ng ml^{-1} With silver enhancement: 1 ng ml^{-1}	73
	Spiked milk sample, orange and apple juice	AuNPs	AuNP conjugated with two different mAbs: F1-51 (BoNT/A HC-specific) and BoB-92-32 (BoNT/B HC-specific)	In 2% and 1% milk BoNT/A: 5 ng ml^{-1} BoNT/B: 10 ng ml^{-1} In diluted apple juice BoNT/A: 25 ng ml^{-1} BoNT/B: 10 ng ml^{-1} No cross-reactivity between BoNT/A and BoNT/B	74
Staphylococcus aureus	Pork, raw chicken, crab meat and inoculated beef, fried chicken, corn flake, cooked rice, noodle	AuNPs	Anti-protein A IgG was conjugated with AuNPs	Sensitivity: 100% with 28 *S. aureus* strains and 23 non-*S. aureus* strains	75
	Naturally contaminated food samples	AuNPs	Anti-protein A IgG conjugated AuNP	Sensitivity: 100% Specificity: 96–100% with 44 non-*S. aureus* strains	76
	Respiratory samples	AuNPs	Monoclonal anti-*S. aureus* antibody conjugated 40 nm colloidal gold particles	10^6 CFU ml^{-1}	77
Staphylococcus enterotoxin B (SEB)	Spiked tap and surface water, apple juice, raw milk, ham extracts, cheese extracts	Sulforhodamine B (SRB)-encapsulating immunoliposomes	Dextran/BSA/rhodamine B isothiocyanate conjugated thiol derivatized anti-SEB antibody	20 pg ml^{-1} (liner range: 0.02–5 ng ml^{-1})	78
	Recombinant SEB	Hollow gold nanospheres (HGNs) with Malachite green isothiocyanate (MGITC) as Raman reporter (Raman-active probe)	Anti-SEB pAb	0.001 ng ml^{-1}	40
Stretococcus suis	Bacteria isolated from diseased piglets, healthy piglets and human patients	AuNPs	AuNP-conjugated antibody against SS2 (serotype-2)	10^6 CFU ml^{-1}	79
	Bacterial culture solution	AuNPs	Colloidal gold coated with pAbs against serotype 2 capsular polysaccharides (CPS)	10^4 CFU ml^{-1} 0.05 µg of CPS	80
Pneumolysin (*Streptococcus pneumoniae*)	Pneumolysin sample	Au@Ag with rhodamine as SERS reporter	Au@Ag with rhodamine as SERS reporter conjugated anti-pneumolysin antibody, PLY-7)	1 pg mL^{-1}	41
Enterobacter cloacae	Simulated water sample	AuNPs	Colloidal AuNPs conjugated with monoclonal anti-*E. cloacae* antibody	10^2 CFU ml^{-1}	81
Enterobacter sakazakii	Spiked infant formulae samples	CNP	Neutravidin labelled CNP to bind with biotin-tagged amplicon	<10 cells of *Cronobacter* sp. per 10 g	82
Leptospira sp.	Human sera	AuNPs	Leptospira specific antibody against broadly reactive leptospiral antigen and colloidal gold-labelled anti-human IgM antibody	Sensitivity: 85.8% Specificity: 93.6%	83

Table 1 (*Contd.*)

Bacterial analyte	Sample used for detection	Type of label	LFIA principle	Sensitivity or LOD	Ref.
	Culture media	AuNPs	Colloidal AuNPs conjugated mouse anti-fluorescein antibody to detect m-LAMP label based biotin/fluorescein labelled LipL32 gene amplicons	Specificity: 100% LOD: DNA concentration 3.95×10^{-1} genomic equivalent per ml	84
Vibrio cholerae serogroup O1 and O139	Culture media	AuNPs	Murine mAb against *V. cholerae* LPS-conjugated AuNPs	Sensitivity: 93–100% (O1), 100% (O139) Specificity: 100% (O1), 98–100% (O139) 10^8 and 10^7 CFU mL^{-1} for O1 and O139, respectively	85
Vibrio cholerae O139	Seafood samples	AuNPs	VC-273 Mab conjugated to AuNPs	10^4 CFU ml^{-1} 1 CFU ml^{-1} with pre-incubation of sample with in alkaline peptone water for 12 hours	86
Vibrio parahaemolyticus	Culture media grown bacterial antigen	CdTe QDs	pAb against *V. parahaemolyticus* conjugated with CdTe QDs; quenching by mAb labelled AuNPs	5.03×10^4 cfu L^{-1}	87
Treponema pallidum (Syphilis)	Serum samples from 8 geographically diverse sites	AuNPs	9 Commercially available rapid syphilis tests	Sensitivity: 84.5–97.7% Selectivity: 84.5–98%	88
Mycobacterium tuberculosis Tuberculosis (TB)	Whole blood and serum spiked with *M. tuberculosis* antigen	AuNPs	40 nm AuNP conjugated with protein-A	5 ng ml^{-1}	89
Listeria monocytogenes	Bacterial culture	AuNPs	AuNP-conjugated nucleotides to detect hlyA mRNA	0.5 pg μl^{-1} of genomic RNA 20 CFU ml^{-1}	90
Listeria monocytogenes	Spiked milk samples and other food samples (including salad, frozen vegetables *etc.*)	CNP	CNP-neutravidin conjugate to bind to biotin modified aptamer	0.1 ng of labelled amplicon 50 pg of *L. monocytogenes* template DNA (approximately 10^5 cells)	91
Helicobacter pylori	Human faecal sample	AuNPs	Mixture of DF2a and IH10b mAb conjugated AuNP	10^4 CFU mL^{-1}	92
Cronobacter spp.	Pure culture and powdered infant formula (PIF)	AuNPs	Biotin-labelled 16s ribosomal DNA of *Cronobacter* sp. detected using streptavidin linked AuNPs	10^7 CFU mL^{-1}	93
Salmonella typhimurium	Bacterial culture derived antigen	Liposome entrapped Methylene Blue (MB)	Thiol derivative of anti-*Salmonella* antibody conjugated with maleimide-derivatized liposomes containing MB	1680 cells	94
Salmonella choleraesuis	Pure culture and spiked whole milk samples	Gold magnetic bifunctional nanobeads (GMBN)	Anti-*S. choleraesuis* mAbs (11D8-D4) conjugated GMBN	Sensitivity: 5×10^5 CFU mL^{-1}	95
Brucella sp.	Bacterial culture	UCP	pAb against *B. melitensis* M55009 covalently coupled with UCP particles	2.0×10^3 to 3.9×10^5 CFU mg^{-1}	96
Pantoea stewartii subsp. *stewartii*	Spiked corn seed samples	Lanthanide (Europium chelate-coated silica nanoparticles)	Anti-Pss antibody conjugated Europium chelate-coated silica nanoparticles	10^4 CFU mL^{-1}	97
Y. pestis and *B. pseudomallei*	Bacterial culture	UCP	mAb against *Y. pestis* and *B. pseudomallei* conjugated UCP	Sensitivity: 10^3 CFU per test	98
Pseudomonas aeruginosa and *Staphylococcus aureus*	Bacterial culture	AuNPs	AuNP-conjugated pAb against *P. aeruginosa* and *S. aureus*	500–5000 CFU mL^{-1} Specificity: 100%	99
E. coli O157:H7 and *Salmonella typhimurium*	Recovered bacteria from contaminated lettuce	AuNP	AuNP-conjugated anti-*S. aureus* and anti-*E. coli* O157 antibody	*E. coli* O157:H7: 1.87×10^4 CFU *S. typhimurium*: 1.47×10^4 CFU After enrichment *E. coli* O157:H7: 1 CFU *S. typhimurium*: 1 CFU	100

Table 2 Comparative study of various viral and protozoal diseases in regard with LFIA-based diagnosis

Disease condition	Causing agent	Laboratory diagnosis	Sensitivity or LOD/ drawback	Type of label	Analyte	Label used	Sensitivity or LOD	Ref.
				LFIA-based diagnosis				
Protozoal								
1. Malaria	*Plasmodium falciparum* (major) Other *Plasmodium* species	Laboratory-based thin blood smear microscopy	Parasitemias of 50 parasites per μL	AuNP	*Plasmodium* lactate dehydrogenase (pLDH)	Colloidal AuNP-labelled pan-specific-anti-pLDH-mAbs	Parasitemias of ≥100 parasites per μL	120
				AuNP	*Plasmodium falciparum* histidine-rich protein 2 (pfHRP-II)	Thermally responsive magnetic nanoparticle (MNP)	10 ng mL^{-1} of pfHRP-II	122
				AuNP	pLDH	AuNP-conjugated anti-pLDH with QR barcodes linked with Google Analytics	10 ng mL^{-1} of recombinant pLDH	123
				AuNP		Micellar Aqueous Two-Phase System (ATPS) with anti-pLDH conjugated AuNP	1 ng μL^{-1}	124
				CNP	Biotin-labelled 18s RNA of *Plasmodium* sp.	Neutravidin labelled CNP to bind with biotin-tagged amplicon	0.3 to 3 parasites per μL	31
Leishmaniasis	*Leishmania infantum*	Skin biopsies, ELISA, Immunofluorescence	Sensitive but time consuming and difficult to operate	AuNP	*Leishmania infantum* kinetoplast DNA	20 nm AuNP-conjugated pAb to recognize anti-FITC antibodies.	0.038 parasites per 1 parasite per 100 μL of DNA sample)	125
Schistosomiasis	*Schistosoma* sp.	Eggs identification in stool, ELISA, microscopy	Time consuming and highly expertise technician and facilities are must	Up-converting phosphor (UCP)	*Schistosoma* Circulating Anodic Antigen (CAA)	Mouse monoclonal anti-CAA antibody 147 coupled to 400 nm UCP reporter particles	0.5 pg mL^{-1}	126
	S. haematobium			UCP	*Schistosoma* CAA	Mouse monoclonal anti-CAA antibody 147-3G4 coupled to 400 nm UCP reporter particles	30 pg CAA per mL serum; (equivalent to about 10 worm pairs)	127
Viral								
Influenza	Influenza virus with different subtypes	HI assay, seroconversion detection between acute- and convalescent-stage samples	HI assay: 92%	AuNP	Hemagglutinin (HA)	AuNP-labelled Mab against HA	0.25 HA units	128 and 129

Table 2 (Contd.)

Disease condition	Causing agent	Laboratory diagnosis	Sensitivity or LOD/drawback	LFIA-based diagnosis				
				Type of label	Label used	Analyte	Sensitivity or LOD	Ref.
				AuNP	Streptavidin-coated AuNPs linked with the biotin moieties incorporated in the middle of the DNA strands	M gene, H1, H3. H5 gene	10^2 copies	130
				AuNP	AuNPs to capture biotin-labelled reverse-transcription loop-mediated isothermal amplification (RT-LAMP)		10 copies	131
				AuNP	Silver growth on AuNP-conjugated anti-Flu A	Flu A antigen, Flu B antigen	Sensitivity and specificity: Flu A – 91.2% and 95.8% Flu B –94.4% and 98%; respectively	132
				AuNP	Anti-nucleoprotein (NP4) MAb and anti-matrix protein (M1) MAb conjugated AuNP (15 nm)	Nucleoprotein and matrix protein	47 $TCID_{50}$ per mL	133
				AuNP	Anti-HA (H3, H5, H7, H9) antibody conjugated AuNP to detect biotin-tagged aptamer captured specific virus	HA	2×10^6 virus particles	134
				Cy5-doped silica nanoparticles	mAb against influenza A nucleoprotein conjugated Silica nanoparticles	Influenza A	250 ng mL^{-1}	135
Hepatitis	Hepatitis virus type-A, B, C, E (HAV, HBV, HCV, HEV)	Liver biopsy	Time consuming with need of skilled technician and well-equipped laboratory	AuNP	Colloidal-gold-labelled antibody against HBsAg	HBsAg, HBeAg	HBsAg – 95% HBeAg – 80%	136
				AuNP	Anti-human-IgM MAb, colloidal-gold-labelled antibody to HEV preincubated with HEV antigen	HEV IgM	93%	137
				AuNP	Colloidal gold-labelled anti-HEV mAb 4B2 and recombinant protein EP2.1	IgM antibody specific to HEV	96.7%	138

opy

Table 2 *(Contd.)*

Disease condition	Causing agent	Laboratory diagnosis	Sensitivity or LOD/drawback	Type of label	Analyte	Label used	Sensitivity or LOD	Ref.
				Fluorescent lanthanide	HCV	Eu^{3+}-chelate conjugated recombinant Multiepitope protein (MEP)	Sensitivity: Secondary antibody assay – 91.4% Double-antigen assay – 95.6%	139
				UCP	Hepatitis B surface antigen (HBsAg)	HBsAg conjugated UCP	60 mIU mL^{-1}	140
				ZnSe/CdSe/CdS/ Cd$_x$Zn$_{1-x}$S/ZnS QDs	HBsAg	HBsAg conjugated QDs	0.05 ng mL^{-1}	141
				Carboxyl-modified CdSe/ZnS QDs	HBsAg	Anti-HBsAg mAb-labelled QB	75 pg mL^{-1}	142
AIDS	HIV	HIV ELISA, HIV viral load test, quantitative PCR	95–100% (~1 ng mL^{-1})	AuNP	HIV-1 p24 antigen	Anti-HIV-1 p24 antibody-selenium colloid based sandwich format with monoclonal biotinylated anti-HIV-1 p24 antibody	25 pg mL^{-1}	143
				AuNP	HIV-1 p24 antigen	Mouse mAb conjugated to super-paramagnetic particles (200–300 nm)	30 pg mL^{-1}	144
				AuNP	HIV-1 RNA	AuNP-labelled probe (partially complementary strand)	10.5–13log$_{10}$ copies per mL (50 copies of *gag* RNA)	145 and 146
				CNP	p24 antigen	Mouse monoclonal anti-p24 mAb108 coupled to CNP	LOD: 50 pg mL^{-1} Sensitivity: 90% Specificity: 100%	147
				Platinum core–shell nanocatalyst (PtNC)	p24 antigen	Anti-HIV-1/2 conjugated PtNCs	0.8 pg mL^{-1}	148
				AuNP	HIV-1 nucleic acid sequence	AuNP-conjugated amplification probe and AuNP-conjugated complementary and detector probe	0.1 nM	149
				Surface-modified AuNP by MGITC as a Raman reporter (Raman-active probe)	HIV-1 nucleic acid sequence	Raman-active probe-conjugated detection DNA sequence	0.24 pg mL^{-1}	150
Adenoviral diseases	Adenovirus	Virus isolation from tissue culture	100% (takes 3–4 weeks)	AuNP	Adenovirus capsid hexon (signal antibody)	Gold colloid-conjugated mouse mAb to adenovirus capsid hexon	72.6% (within 10 minutes)	151

LFIA-based diagnosis

Table 2 (Contd.)

Disease condition	Causing agent	Laboratory diagnosis	Sensitivity or LOD/drawback	Type of label	Analyte	Label used	Sensitivity or LOD	Ref.
				AuNP	Recombinant HA of H5N1	mAb 25/2 conjugated AuNP	250 ng ml^{-1} without amplification 0.5 ng ml^{-1} with silver amplification	152
				AuNP (later dissolved, collected and GSH capped CdTe QDs added for fluorescent detection)	Avian influenza virus (AIV)	AuNP-conjugated AIV mAb	0.09 ng ml^{-1} Sensitivity: 100% Specificity: 88.2%	153
WNV infection (mostly asymptomatic)	Western Nile virus (*Flaviviridae* family)	WNV IgM/IgG capture (MAC) ELISA	100% (takes 2–3 days)	AuNP	WNV antigen (protein E)	Colloidal gold particles conjugated flavivirus specific mAb (6B6C-1)	95–100% agreement with results from CDC WNV IgM/IgG ELISA (within 15 minutes)	154 and 155
Dengue	Dengue virus (DENV)	Virus isolation, ELISA, RT-PCR	1–10 infectious virus particles, 1–100 PFU ml^{-1} (PCR) (takes days to weeks)	AuNP	NS1 dengue antigen, anti-dengue IgM and IgG	Colloidal gold-labelled specific mAbs against dengue NS1 antigen, IgM, IgG, or IgA	90–100%	156–163
				AuNP	Dengue specific IgG	Streptavidin conjugated 40 nm AuNPs	—	164
Chikungunya	Chikungunya virus (CHIKV)	Virus isolation, RT-PCR	Relative sensitivity 100% with PCR	AuNP	Chikungunya envelope proteins (E1, E2, E3), CHIKV specific IgM	Colloidal gold-conjugated anti-IgM antibody against CHIKV specific IgM and CHIKV recombinant envelope protein in test line	90–100% (arguable as per multiple studies)	165–169
Herpes Simplex Virus (HSV) infection	HSV-2	Virus isolation, RT-PCR, ELISA	Relative sensitivity 95–100% with ELISA	AuNP	HSV-2 specific IgG	Colloidal gold-conjugated anti-IgG antibody with gG1 and gG2 in pre-absorption line and test line respectively	Sensitivity: 100% Specificity: 97.3%	170
Newcastle disease	Newcastle disease Virus (NDV)	Hemagglutination inhibition (HI) assay, agar gel immunodiffusion (AGID), ELISA, RT-PCR	Highly sensitive and selective	AuNP	Purified NDV	40 nm AuNP conjugated with anti-NDV-6C4 mAb	2×10^{-12} M	171
Ebola	Ebola Virus (EBOV)	Whole antigen ELISA, virus isolation in cell culture	Sensitive with prolonged time consuming	AuNP	EBOV Glycoprotein (EBOV-GP$_{1-649}$)	Anti-human IgG conjugated AuNP	Sensitivity: 100% Selectivity: 98%	172
				Fe$_3$O$_4$ MNPs	EBOV glycoprotein (EBOV-GP)	Anti-EBOV-GP (4G7) conjugated MNPs	1 ng ml^{-1}	173

Table 2 (Contd.)

| Disease condition	Causing agent	Laboratory diagnosis	Sensitivity or LOD/ drawback	LFIA-based diagnosis Type of label	Analyte	Label used	Sensitivity or LOD	Ref.
Norovirus	Norovirus	Microscopy, ELISA, RT-PCR	Reduced clinical specificity, expensive	Biotin-labelled anti-Norovirus antibodies linked with streptavidin-biotin conjugated AviTag M13 phage with HRP/anti-M13 antibody	Virus-like particles (VLPs) from GI.1 (first recognized Norovirus)	Biotin-labelled anti-Norovirus antibodies linked with streptavidin–biotin conjugated AviTag M13 phage with HRP/anti-M13 antibody	10^7 VLPs per ml	174
Dengue, Zika	DENV and Zika virus (ZIKV)	PCR amplification of specific genes, virus isolation culture, ELISA	Hard to distinguish from each other based on isolation and ELISA, expensive, cross-reactivity with other viruses of Flaviviridae family	AuNS with 1,2-bis(4-pyridyl)ethylene (BPE) and 4-mercaptobenzoic acid (MBA) as Raman reporter	DENV-NS1 ZIKV-NS1	Anti-DENV NS1 and anti-ZIKV NS1 conjugated gold nanostars with different Raman reporters	DENV – 7.67 ng ml^{-1} ZIKV – 0.72 ng ml^{-1}	43
				AuNP	DENV-NS1 ZIKV-NS1	Serotype-specific DENV nanoparticle-mAb conjugates and ZIKV nanoparticle-mAb conjugates	Sensitivity/specificity: 0.76 to 1.00 for DENV 1–4 and the pan-DENV; 0.81/0.86 for ZIKV respectively	175
AIDS, Hepatitis C, Hepatitis A	HIV, HCV, HAV	ELISA, Viral Load Test, quantitative PCR, liver biopsy	Co-infection of HIV and HCV	AuNP	Proteinticles (P) P_{HIV}-gp41, p24 P_{HCV}-511p, c100p, c22p, and c33c P_{HAV}- E1, E2, E3	Protein-A conjugated AuNP	Sensitivity: 100%	176
Dengue, yellow fever, Zika	DENV, yellow fever virus (YFV), ZIKV			AgNP	DENV NS1 protein, yellow fever virus NS1 protein, and EBOV, Zaire strain glycoprotein GP	AgNP conjugated anti-dengue NS1, anti-YFV NS1, anti-EBOV-GP mAb	150 ng ml^{-1}	177
Kaposi's sarcoma-associated herpesvirus (KSHV) and Bacillary Angiomatosis (BA)	HSV, *Bartonella* sp.			AuNP modified with MGITC as Raman reporter (Raman-active probe)	DNA sequences associated with KSHV and BA	Thiol-modified DNA conjugated SERS active AuNPs	KSHV: 0.043 pM and BA: 0.074 pM	178
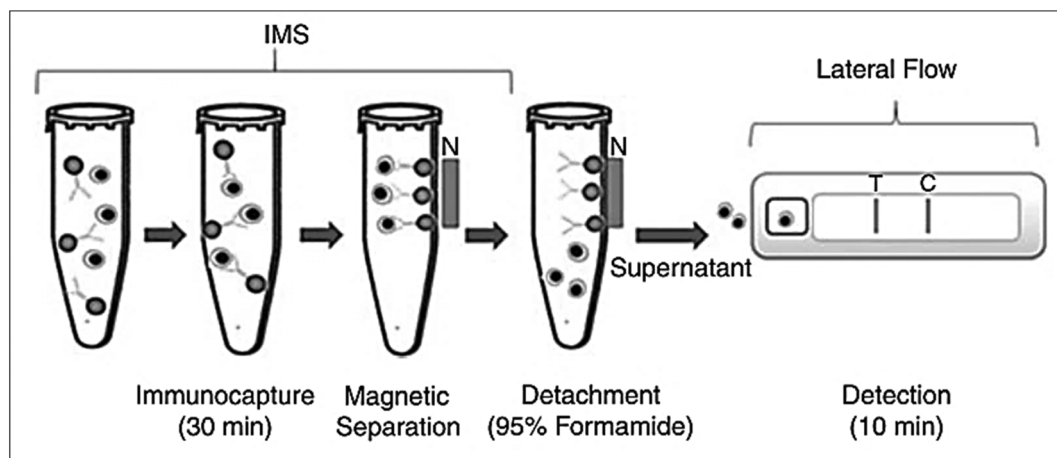
Fig. 4 Principle of IMS and LFIA for the detection of *Bacillus anthrax* spores. Anti-spore antibodies coupled with COOH-magnetic beads are used for immunocapture. Magnetic separation is achieved by using magnetic field. The spores are recovered using formamide and EDTA and are used directly in the LFIA device. Reprinted (adapted) with permission from ref. 62. Copyright (2009) John Wiley and Sons.

family members are known for causing various water-borne diseases. They produce various endotoxins and exotoxins that cause the pathogenesis of the infection by interacting with the digestive juices, resulting in enormous water loss from the body. Botulism is a fatal infectious disease caused by a neurotoxin botulinum (BoNT) produced by *Clostridium botulinum* and is capable of causing paralytic illness in human when found even in a very small amount in food.[108] The toxin is classified in 7 antigenic types (A–G) based on their absence of cross-neutralization, *e.g.* anti-G antitoxin does not neutralize toxin types A–F.[109] The detection of BoNT/D by sandwich format LFIA has been established using AuNPs as a label with a detection limit of 50 pg mL^{-1}.[72] A similar strategy was used for BoNT/A detection, where mAb against BoNT/A conjugated with AuNP was used. This detection showed no cross-reactivity with BoNT/B or BoNT/E when a silver enhancement reagent was used to amplify the signal generated from colloidal gold. The detection limit for this LFIA strip was found to be 1 ng mL^{-1}.[73] The simultaneous detection of BoNT/A and BoNT/B was reported by using separate mAbs with a high affinity and specificity for the two mentioned serotypes.[74] Another bacterium, *Staphylococcus aureus*, is the leading cause of food poisoning, especially in processed and canned foods.[110] LFIA based on a sandwich format was developed for detecting *S. aureus* in processed food (pork, beef, fried chicken).[75] The sensitivity of the immunochromatography test was found to be 100% when tested with 28 *S. aureus* and 23 non-*S. aureus* strains. *Stretococcus suis* has been identified as a causative agent of meningitis and endocarditis in humans.[111,112] A LFIA strip based on colloidal AuNPs has been developed against serotype 2, which is the most common and pathogenic both to humans and pigs.[79] The sensitivity of the immunochromatography strip was found to be 10^6 CFU mL^{-1}. A recent breakthrough in detecting *Enterobacter cloacae* was achieved by using an IMS of *E. cloacae* from a sample and then detecting it with monoclonal anti-*E. cloacae* antibody conjugated with col-

loidal AuNPs.[81] *E. cloacae* can induce various pathogenic conditions including respiratory tract infection, urinary system infection, skin and soft tissue infection and septicaemia.[113,114] The LFIA test strip showed 10^2 CFU mL^{-1} of *E. cloacae* detection with IMS, which showed a 10 times lower LOD than that of the direct detection. mAb against *Vibrio cholerae* subtype O1 and O139 was used with colloidal gold for the multiplexed detection of the subtypes of *V. cholerae*. The detection limit of the device was found to be 10^8–10^7 CFU mL^{-1}.[85] There are several toxins (like mycotoxins and aflatoxins) produced by various bacteria or fungi, and some specific types of bacterial infection (like *Listeria* sp. infection) are extensively described in other reviews.[23,115–119]

3.2 LFIA for detecting protozoal infection

The nanoparticle-labelled simple lateral flow-based tool can identify labels of a whole pathogen. For example, commercially available rapid test strips for malaria detection are capable of detecting *P. falciparum* and other *Plasmodium* species at levels of ≤500 parasites per μL and ≤5000 parasites per μL, respectively. Also, as per WHO guidelines, some rapid test strips are available for use in the market (CareStart™ Malaria test, OptiMAL-IT™) that can detect *Plasmodium* very efficiently with parasitemias of ≥100 parasites per μL.[120] In other standard rapid diagnostic tests, *P. falciparum* dehydrogenase and Histidine-rich Protein 2 (*pf*HRP II) are used as species-specific markers for *P. falciparum*.[180] OptiMAL-IT's™ design is based on the detection of pLDH (plasmodium lactate dehydrogenase) using pan-specific-anti-pLDH-mAbs labelled with AuNP.[181] NTA-functionalized gold and AgNP has recently been exploited for the detection of *pf*HRP II mimics, specifically without any cross-reactivity with human serum proteins. NTA is a chelating agent that has a high affinity towards histidine (the dissociation constant (K_d) value is in the micromolar range[182]). At a low pH, NTA-NPs do not show aggregation with human serum proteins, which enables further development to
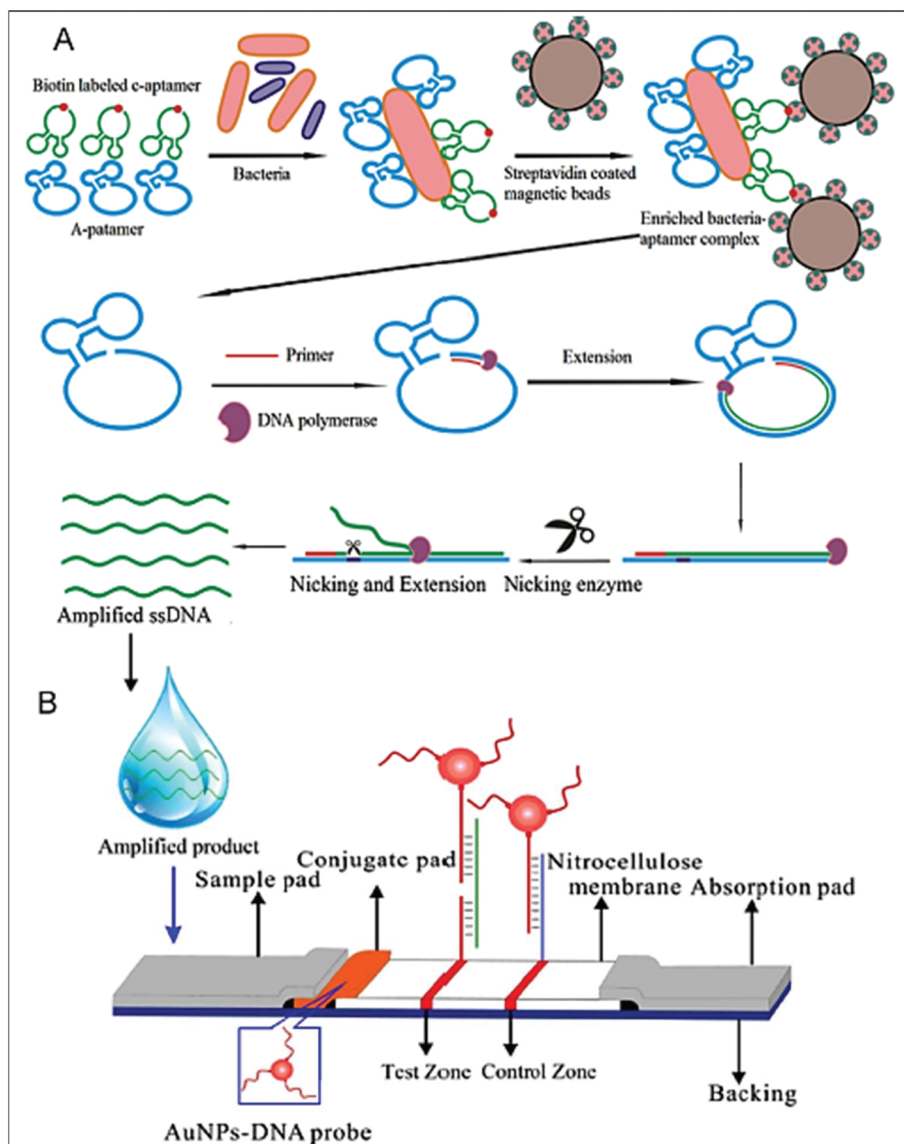
Fig. 5 Schematic design of the aptamer-based detection of *Salmonella enteritidis*, A. magnetic separation using a streptavidin-coated magnetic bead. The biotin-labelled aptamer bound bacteria is detected by streptavidin interaction and magnetically separated, followed by strand-displacement amplification leading to the production of an amplified sample containing ss DNA, B. the LFIA strip containing the ss DNA-AuNP probe for detection. Reprinted (adapted) with permission from ref. 59. Copyright (2014) Elsevier.

detect *pf*HRP-II in human serum or saliva.[121] On the other hand, nucleic-acid-based lateral flow assay for detecting malaria is also widely studied.[180] A recombinase polymerase amplification (RPA) strategy has also been used to design a LFIA device. The RPA amplicon was labelled for the detection by a tag-specific antibody in the control and test lines. The conjugate pad contained AuNPs for visualizing colour formation (Fig. 8). This gave a high species-specific result with high sensitivity and specificity (100%). The detection limit was found to be 100 fg of genomic *P. falciparum* DNA (equivalent to a sensitivity of 4 parasites per reaction).[179] Thermally responsive MNP is also used in studies to concentrate and aggregate a greater amount of *pf*HRP II as a pre-step before

putting the sample on the strip (Fig. 9). Here, the sample was treated with a biotinylated antibody, which formed aggregation when treated with heat after the addition of streptavidin-pNIPAm-AuNP, pNIPAm MNP and free pNIPAm polymer. The sample was then subjected to a magnetic field for separating out the mixed AuNP/MNP aggregates and was then re-dissolved in a cold buffer for enrichment.[122] 10 ng mL^{-1} of pfHRP-II detection was achieved using this method of enrichment. A very recent report on pLDH detection using a LFIA platform was successfully implemented on the Google Analytics platform by using a QR barcode for positive, negative and invalid results from the device (Fig. 10). The cross-platform data acquisition could store a very large amount of data from the
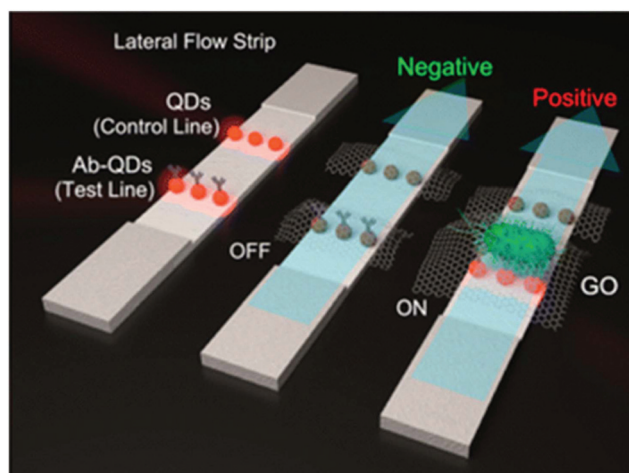
Fig. 6 Schematic representation of the working mechanism of GO quenching of fluorescence in the absence (OFF mode) and presence (ON mode) of bacteria. Reprinted (adapted) with permission from ref. 57. Copyright (2015) American Chemical Society.

device and was readable by a smartphone.[123] The QR codes were initially set as "Blank" with both the QR codes incomplete (deactivated). Whether the test result is positive, negative

or invalid, it can produce three different types of QR code, which can be scanned using a smartphone camera to obtain data about the test.

Schistosomiasis is a parasite disease caused by *Schistosoma*, a blood-dwelling fluke worm.[183] UCP has been employed for the detection of circulating anodic antigen (CAA), a biomarker of *Schistosoma*. The detection limit achieved by using UCP was 0.5 pg mL^{-1} of CAA[126] and the robustness of the same method was improved by using dry (lyophilized) reagents with a detection limit of 30 pg mL^{-1}.[127]

3.3 LFIA for detecting viruses and viral infections

Some other remarkable studies demonstrated the detection of virus and viral protein using LFIA devices. The H9 subtype of AIV was successfully detected using a LFIA strip developed using two different mAbs for test line and control line separately with a sensitivity of 0.25 hemagglutinin units in less than 10 minutes. The antibody 4C4 against HA was labelled with AuNP and the antibody 4D4 against nucleoprotein and applied on the test line.[128] A similar type of approach was used to detect the H5 subtype (H5N1) without any cross-reactivity with the H1–H4 or H6–H14 subtypes.[184] In comparison with the hemagglutination (HI) assay and agar gel immunodiffusion assay (AGID), a gold-immunochromatographic (GICA) test strip
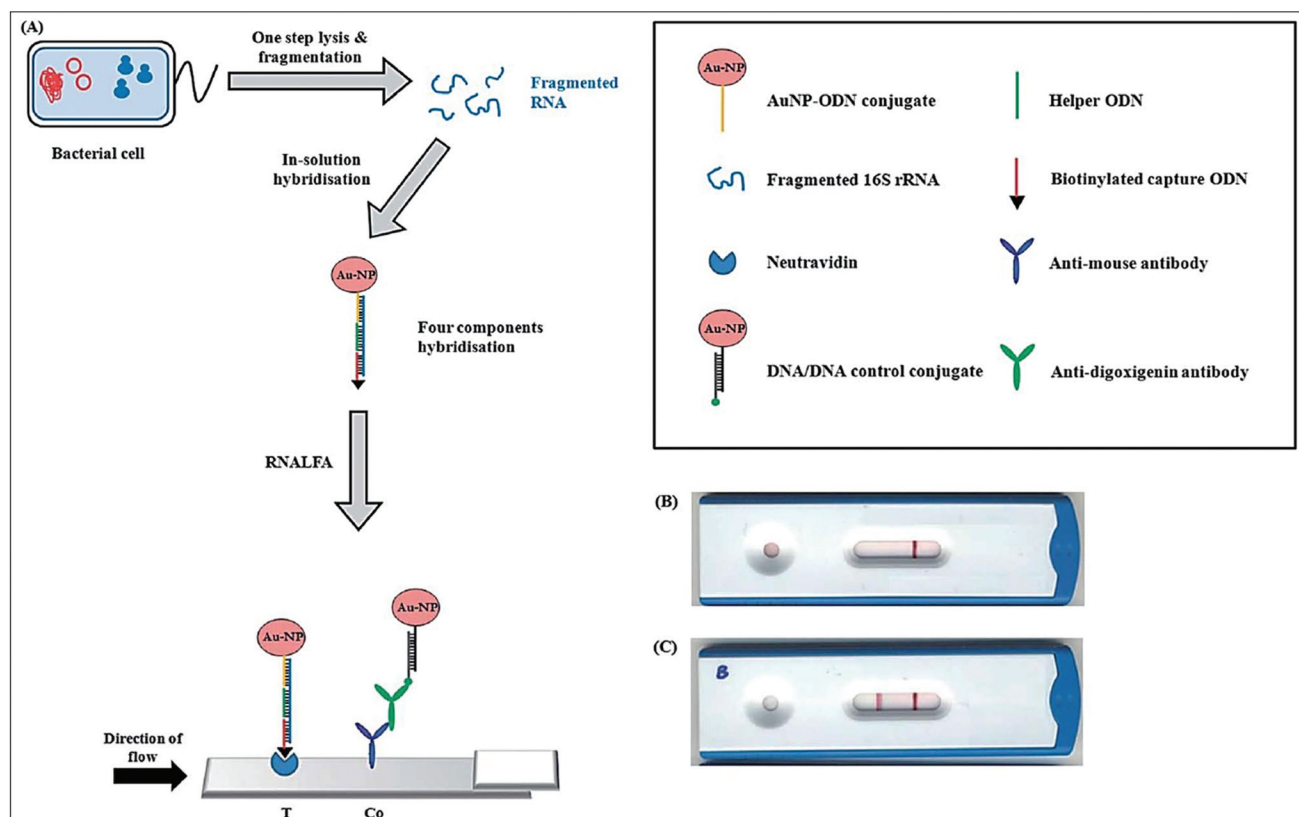

Fig. 7 Principle of the ribonucleicacid lateral flow assay (RNALFIA); A. lysis and subsequent fragmentation of *E. coli* cells produces fragmented RNA, which is required for the four component hybridization with the AuNP-oligodinucleotide (ODN) conjugate, biotinylated capture ODN and a helper ODN. This hybridized assembly is then applied on the lateral flow strip with neutravidin immobilized at the test line and anti-mouse antibody at the control line. Reprinted (adapted) with permission from ref. 105. Copyright (2014) Royal Society of Chemistry.
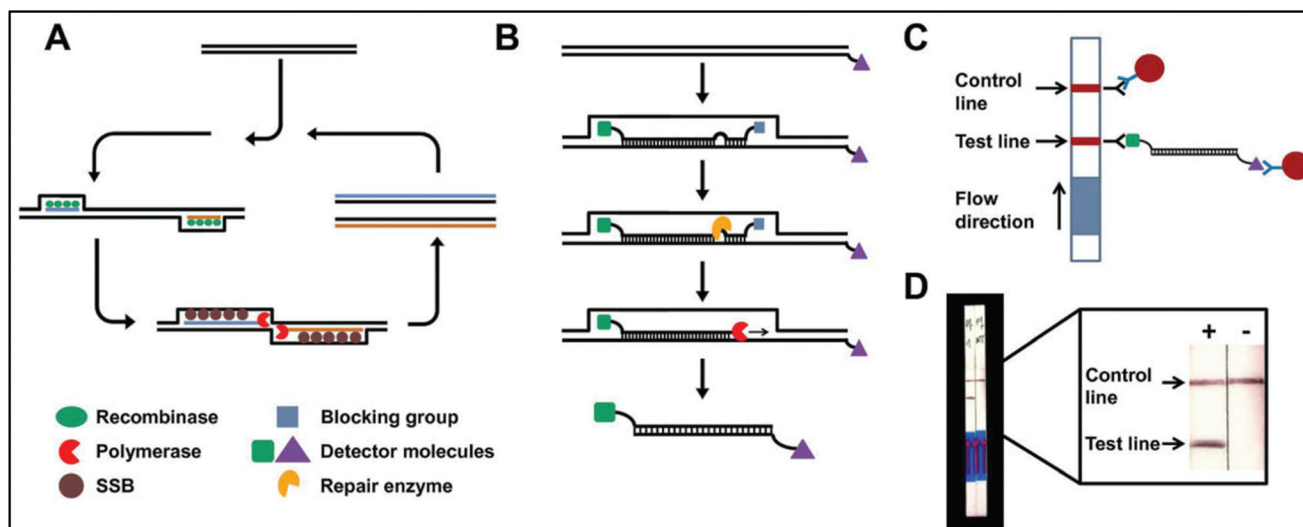
Fig. 8 Schematic representation of an RPA-mediated LFIA device. A. Reaction principle, B. modified-probe labelling, C. detection mechanism, D. observation of positive and negative results. Reprinted (adapted) with permission from ref. 179. Copyright (2014) BioMed Central Limited.
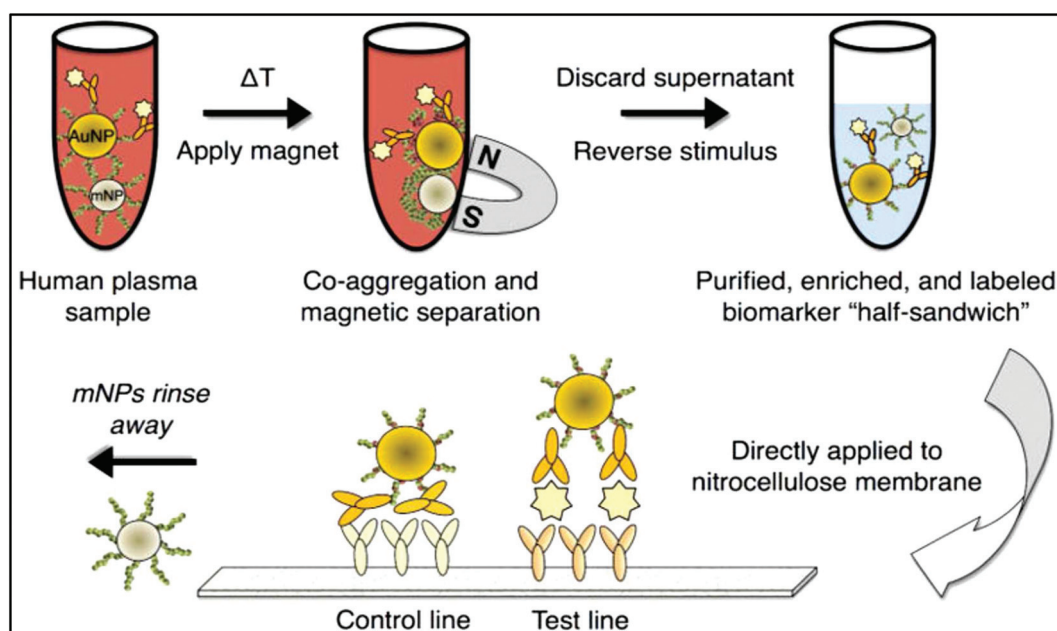

Fig. 9 Schematic diagram of magnetic-enrichment LFIA. Reprinted (adapted) with permission from ref. 122. Copyright (2012) American Chemical Society.

showed high sensitivity and specificity.[185] The rapid detection of HBV and HEV[138] was largely achieved through the immuno-chromatography assay principle. There are various commercial kits available for HBV and HEV rapid detection (like ACON, Atlas Medical, Dima, Cortez, Blue, Intec, HEPACARD, Assure).[136,137,186,187] They provide excellent screening with comparable sensitivity and specificity with PCR.[188] A sensitivity and specificity both ranging between 97.5% and 98.3% have been observed with a 240 patient serum sample. The use of fluorescent QDs as labels are advantageous as they have a high quantum yield, tuneable fluorescent emission spectra and a greater lifetime. Carboxyl-modified CdSe/ZnS quantum beads (QBs) as labels have shown a detection limit of hepatitis B surface antigen (HBsAg) in the picograms per mL range.[142] The detection platform comprised anti-HBsAg mAbs conjugated with QBs. The detection limit achieved by this method was 75 pg mL^{-1}.

Several LFIA devices have been designed to detect DENV in blood or saliva samples. Commercial kits for detecting DENV are designed: (a) to detect the dengue antigen NS1 at the early
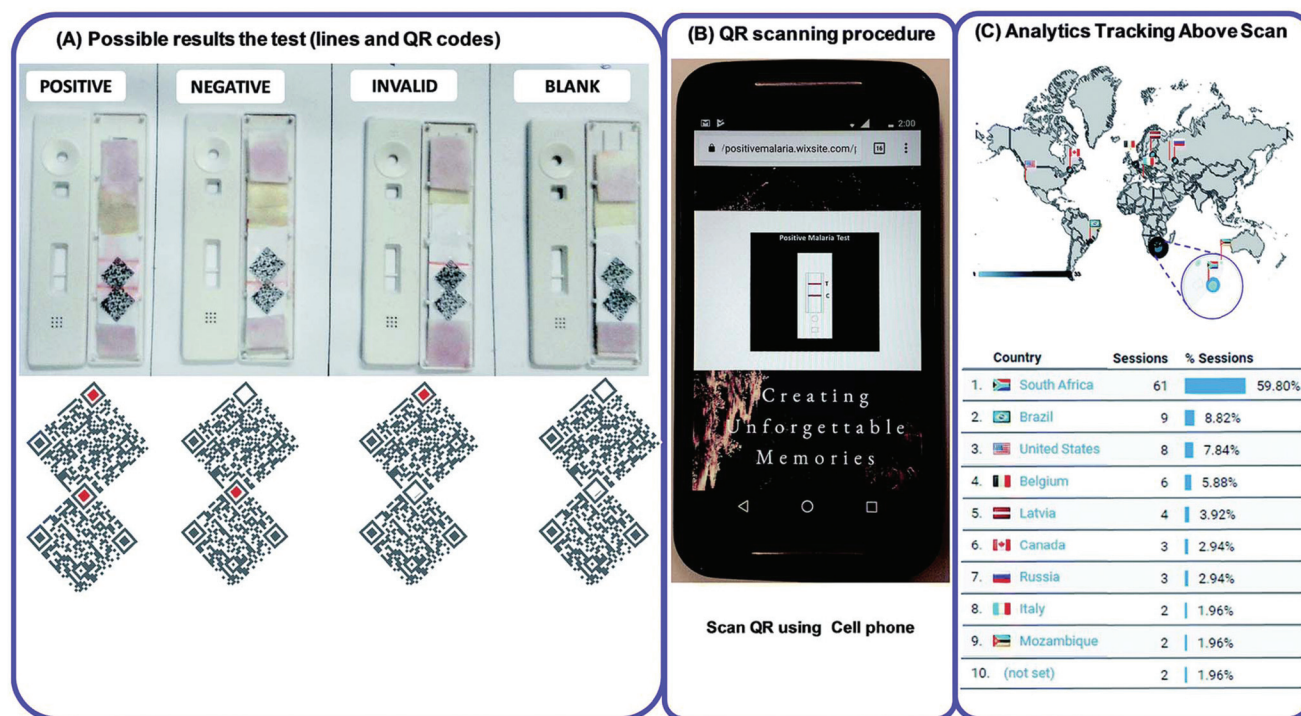
Fig. 10 (A) QR code generation for positive, negative, blank and invalid tests. (B) QR scanning procedure by using a cell phone. (C) Statistical Google analytics real-time data with details like number of users, location, duration and results (positive, negative or invalid). Reprinted (adapted) with permission from ref. 123. Copyright (2017) Royal Society of Chemistry.

stages of infection (Panbio Dengue Early Rapid NS1, SD Bioline Dengue NS1 Ag, BIORAD Strip), (b) to detect anti-dengue IgM and IgG (Panbio Dengue Duo Cassette and SD Dengue IgG/IgM, Merlin IgM, Biosynex IgM, Merlin Dengue Fever IgG and IgM combo device) or (c) to detect both antigen and IgG/IgM (BIOLINE Dengue Duo NS1antigen and IgG and IgM Combo Device).[156–163] For improving the specificity and sensitivity of the test, several other approaches have been implemented. The detection of dengue specific IgG in salivary fluid using a stacking flow platform enabled the detection of DENV in a completely non-invasive sample collection platform (Fig. 11).[164] As shown in Fig. 11, the device was fabricated using two flow paths, one called the sample pad and the other one the reagent pad. The sample pad was introduced with spiked salivary samples and the reagent pad was supplied with protein-G conjugated 40 nm AuNPs. On the other hand, the specific detection of anti-dengue IgM from a blood sample was achieved by using a protein-G coated membrane, which selectively eliminated IgG from the sample.[189] Chikungunya is another viral disease that has been predominantly seen around the world over the years.[190–192] SD Bioline Chikungunya IgM and OnSite Chikungunya IgM Combo Rapid Test are two commercially available immunochromatography-based lateral flow devices that have been approved by the European Commission. Both of these LFIA devices are designed to detect chikungunya-specific IgM present in blood, where recombinant structural proteins from the chikungunya envelope are conjugated with colloidal gold particles for the
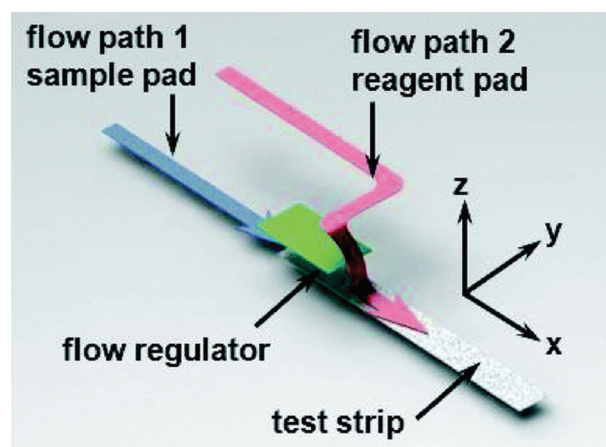

Fig. 11 Schematic illustration of the stacking flow immunoassay device. Reprinted (adapted) with permission from ref. 164. Copyright (2015) Royal Society of Chemistry.

detection. SD Bioline Chikungunya IgM was tested with 407 samples with a sensitivity and specificity of 97.1% and 98.9%, respectively,[165] while the OnSite Chikungunya IgM Combo Rapid Test showed a 90.3% sensitivity and 100% specificity (both are relative to MAC-ELISA results) with 93 samples.[166] Surprisingly, multiple field studies have been conducted based on these two LFIA devices but have shown very poor performances.[167–169,193] The first EBOV outbreak took place in

West Africa in 2014 [194] with a fatality rate of 70.8%.[195] The rapid diagnosis of EBOV by using LFIA as a POC tool showed a 100% sensitive detection of IgG antibodies against EBOV Glycoprotein (EBOV-GP$_{1-649}$).[172] A detection limit of 1 ng ml^{-1} of EBOV-GP was achieved by using Fe$_3$O$_4$ MNPs conjugated anti-EBOV-GP (4G7).[173] Recently, a multiplexed disease diagnostic strip was designed to detect three different types of viruses causing Dengue, Yellow fever and Ebola.[177] The label used in this study comprised AgNPs with three different sizes and having different colours. These nanoparticles were conjugated to antibodies specific for a particular disease and used for three different test lines to easily identify the specific virus present in the sample with a detection limit of 150 ng ml^{-1} (Fig. 12). Multiplexed as well as the SERS-based enhanced detection of Dengue NS1 antigen and Zika NS1 antigen was also investigated. Very low detection limits of 7.67 ng mL^{-1} and 0.72 ng mL^{-1} for DENV NS1 and ZIKV NS1, respectively, were achieved by using two different Raman reporters conjugated gold nanostars.[43] The detection of rabies virus in rabies endemic countries is often challenging as they often lack the infrastructure and funds to employ the gold standard for definitive diagnosis of rabies infection, i.e. the fluorescent antibody test (FAT).[196] Instead, for the low-cost and rapid detection of rabies infection, two types of immunochromatography test kits were developed by using mAbs, which can recognize epitope II and III of the nucleoprotein of the virus.[197] The specificity and sensitivity for type 1 (a single mAb was used) and type 2 (two different mAbs were used) were found out to be 88.9%, 95.5% and 100%, 93.2% respectively. Furthermore, the assay showed no cross-reactivity with other

common canine-pathogenic viruses. The commercially available immunochromatography strip for rabies virus detection was evaluated and the specificity and sensitivity were found to be 100% and 91.66%, respectively, with brain samples from different rabies suspected animals.[198–201]

As per WHO, around 30% of the HIV affected people are unaware of their infectious status. Critical gaps exist in many developing countries in HIV prevention, diagnosis and treatment.[202] For that, in low resource settings, LFIA devices as a POC tool can serve this gap by providing faster and simpler detection platforms. WHO criteria for using such POC must meet the ASSURED (Affordable, Sensitivity and Specificity, User-friendly, Rapid and robust, Equipment-free, Deliverable) requirement.[203] Determine HIV-1/2 (Abbott Laboratories) is a commercially available selenium colloid based immunochromatographic rapid test strip that uses a sandwich format to detect anti-HIV-1 or anti-HIV-2 antibodies present in the patient's serum or plasma or from the whole blood sample.[204] The test was evaluated by various groups. Samples from various locations around the world were tested and the test correctly predicted the results from the samples with a 100% sensitivity.[205–207] Alere Determine HIV-1/2 Ag/Ab Combo is an FDA-approved rapid LFIA strip that is used commercially for HIV diagnosis.[208] The principle is the same as that of the previously described kit (Determine HIV-1/2 by Abbott Laboratories) with the only difference being the analyte; here the analyte is the p24 antigen as well as antibodies to HIV-1 and HIV-2.[143] Some of the other commercially available HIV detection kits have also been evaluated and in most cases the sensitivity was found to be nearly 100% with serum or plasma
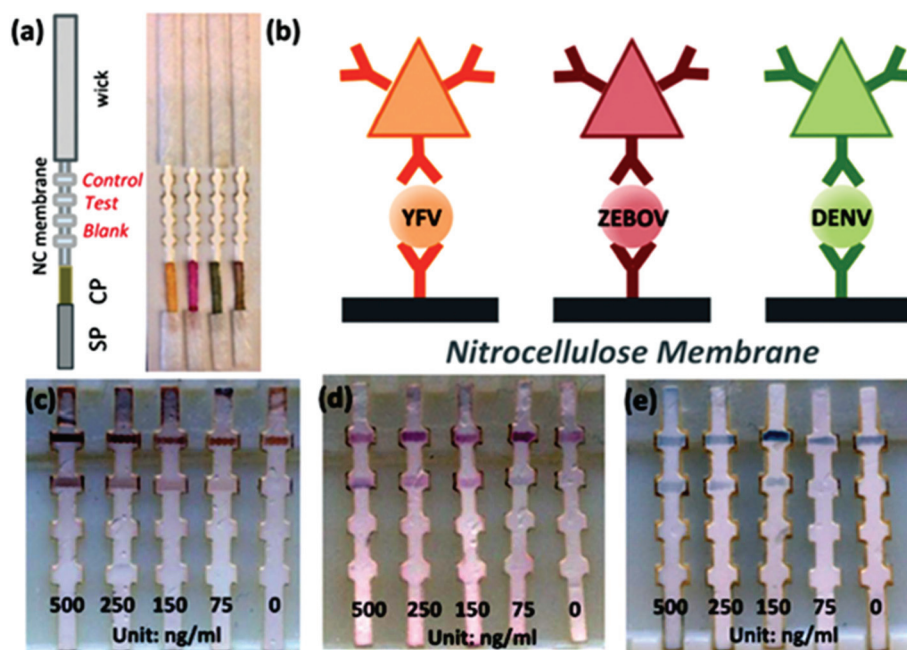

Fig. 12 a. Lateral flow strip, b. schematic of the sandwich assay showing different coloured antibodies conjugated with mAbs specific to YFV NS1, ZEBOV GP, DENV NS1 (from left to right), c–e. Limit of detection of the LFIA strip. Reprinted (adapted) with permission from ref. 177. Copyright (2015) Royal Society of Chemistry.

samples.[145,206,207,209–211] HIV-1 p24 detection by the magnetic immuno chromatographic test (MICT) by using super-paramagnetic nanoparticles[212] has also been reported.[144,213] The magnetic moment of the super-paramagnetic particles that serve as a label for the assay has been detected using a cost-effective instrument involving multiple coil sensors arranged as a gradiometer to form a dedicated magnetic assay reader system.[144] A recent report on the detection of p24 showed the use of PtNCs, which serve as a catalyst in the LFIA platform. The signal amplification by using this method showed a 100-fold catalytic enhancement and it was thus able to detect 0.8 pg ml^{-1} of p24.[148] Amplified HIV-1 RNA detection[145] by NALFIA using AuNPs showed a resolution of 10.5–13log$_{10}$ copies per mL over a linear range and 50 copies of HIV *gag* RNA when coupled with nucleic acid sequence-based amplification (NASBA).[146] The assay was designed to detect an amplified 142 bp RNA sequence by an AuNP-labelled partly complementary nucleotide strand. When a sample containing the RNA sequence is present, it binds with the AuNP-labelled probe as well as with nucleotide sequence present in the nitrocellulose membrane of the strip. After washing the strip, gold enhancement is done for signal amplification and for improving the LOD (Fig. 13). SERS-based enhancement has been done for HIV nucleic acid detection. A detection limit as low as 0.24 pg mL^{-1} for HIV-1 DNA was achieved by using MGITC-modified AuNSs as the probe.[150] Some opportunistic infections of HIV, like cryptococcosis caused by *Cryptococcus* sp., were also diagnosed and evaluated using a LFIA.[8,214]

A significant cause of diseases in respiratory tract and eye (Pharyngoconjunctival fever) is the human adenovirus. The adenovirus antigen immunochromatographic test is being developed that can detect the virus within 10 minutes from pharyngeal swab specimen.[151] The IC test showed a sensitivity of 72.6% and a specificity of 100% with serotypes 1, 2, 3, 5 and 7. Other studies have also shown comparable sensitivity with the previous results.[215,216] Another mosquito-borne virus, Western Nile virus is a human neuropathogen commonly found in Africa, Asia, Europe and the Middle East.[217,218] Though there

are many immunofluorescence assays and as MAC-ELISA-based techniques are available for laboratory screening of WNV, they show 4% to 10% cross-reactivity with other flaviviruses.[219–221] A solid-phase immunochromatographic strip with colloidal gold particles as the label RapidWN™ was developed in 2007.[154] The LFIA showed a high sensitivity and selectivity of 98.8% and 95.3%, respectively, which is comparable with the gold standard IgM-based EIA.[155] NDV belongs to the family *Paramyxoviridae*. A LFIA device for the detection of NDV was achieved by using 40 nm AuNPs conjugated with anti-NDV-6C4 mAb.[171] Gold enhancement on the immobilized AuNP-antibody conjugate showed an increased detection limit by a factor of 10–100 fold. An unconventional method to detect the norovirus used M13 bacteriophage nanoparticles as reporters instead of coloured latex or AuNPs. Here, the M13 bacteriophage was used to selectively bind to biotin-labelled anti-norovirus antibodies by biotin–streptavidin–biotin conjugation. Then, the horseradish peroxidase (HRP) conjugated anti-M13 antibody was bound to the bacteriophage. TMB was used then as a chromogenic substance to develop colour.[174] The detection limit achieved by using this system was 10^7 VLPs per ml.

Over the years, LFIA devices have been improved by various means, such as by using a two-dimensional paper flow network,[222,223] installing an organic light emitting diode (OLED) with filters,[224] multiplexing the assay with two or more analytes,[225] as hand-held devices (including smartphone apps) for the quantitative detection of analytes,[100,123] enzyme-based signal amplification[148] and gold- or silver-based signal amplification.[132,152,226] The two-dimensional paper flow system has shown controlled release from patterned, dried reagents, which allows the fabrication and implementation of complex and multiplexed flow patterns (like the flow of reagents for gold enhancement) that must not mix with each other before flowing through the strip by capillary action.[222] These amplification strategies were applied to improve the sensitivity of the detection device. Further, the sensitivity for the detection of fluorescence coming from QD labels was improved through the use of an OLED. This enabled certain advantages over con-
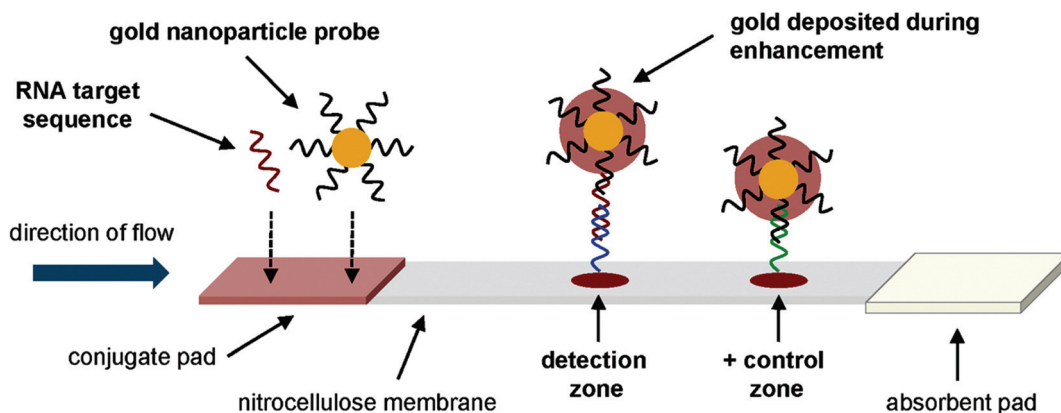

Fig. 13 Schematic design of a lateral flow assay to detect amplified HIV-1 RNA. Reprinted (adapted) with permission from ref. 146. Copyright (2012) Public Library of Sciences (PLOS).

ventional LEDs, such as flexibility and a 7 times improvement over the conventional LFIA device in the detection of influenza as a proof of concept.[224]

4. Conclusion and outlook

This review summarizes the analysis and diagnosis of infectious diseases by LFIA with nanoparticles used as a label. We have seen various pandemics and epidemics around the globe caused by various infectious diseases; so, it is of utmost importance to diagnose infectious diseases and their causative agents as early as possible. This can not only lead to the deployment of early preventive measures but can also help to contain the infection from spreading. Different methods can detect either these infection causing pathogens or their products, in which the lateral flow assay approach provides several advantages. This method of diagnosis is simple, rapid, cost-effective and does not need any specialized persons or training to be operated, thus it can serve as a point-of-care (POC) testing device. Different labels are used, of which colloidal AuNP is the primary label for visualizing and/or quantifying the infection load. AuNP is comparatively easy to prepare, stable and can be readily tuned depending on the type of application. Another advantage of the lateral flow assay is that different analytes can be tested at the same time, which makes LFIA devices multi-parametric. Several LFIA-based devices have been commercialized for the diagnosis of infectious disease and further extensive research is underway to enhance the signal produced from the device with several techniques that can be applied, such as silver enhancement, SERS and magnetic enrichment.

Although LFIA devices enjoy great application already, there are still some limitations associated with LFIA-based devices. The selectivity and signal generation of these devices often hugely depends on the type of sample, its condition and preparation, the volume of the sample, pH, amount of analyte present and the weak interaction forces between the analyte and recognition element. Some of the strategies described here are experimental only so far with the target analyte under controlled conditions. This may affect the outcome of the device's performance in real samples from a patient. To overcome this, present research is focussed more on making LFIA devices more feasible, less dependent on the sample preparation processes, with a shorter incubation time and quantitative result generation. Further, for analytes present in a very low concentration in the sample of interest, a pre-concentration or enrichment step is generally performed. This makes LFIA not suitable for POC applications. To overcome this hurdle, methods such as catalytic enhancement and SERS-based detection are being employed to achieve better sensitivity.

Abbreviations

AgNP(s)	Silver nanoparticles(s)
AIDS	Acquired immunodeficiency syndrome
AIV	Avian influenza virus
AuNP(s)	Gold nanoparticle(s)
BoNT (A/B/C/D/E)	Botulinum neurotoxin (A/B/C/D/E)
CAA	Circulating anodic antigen
CFU	Colony forming unit
CNP(s)	Carbon nanoparticles(s)
CPS	Capsular polysaccharide
DENV	Dengue virus
ds	Double stranded
EBOV	Ebola virus
EHEC	Enterohemorrhagic *E. coli*
EIA	Enzyme immunoassay
ELISA	Enzyme-linked immunosorbent assay
EPEC	Enteropathogenic *E. coli*
FAT	Fluorescent antibody test
GO	Graphene oxide
H(A/B/C/E)V	Hepatitis (A/B/C/E) virus
HA	Hemagglutinin
HBeAg	Hepatitis B envelope antigen
HBsAg	Hepatitis B surface antigen
HI	Hemagglutinin inhibition
HIV	Human immunodeficiency virus
HRP	Horseradish peroxidase
HSV	Herpes simplex virus
IMP	Immunomagnetic particle
IMS	Immunomagnetic separation
LFIA	Lateral flow immuno assay
LPS	Lipo-polysaccharide
mAb(s)	Monoclonal antibody(ies)
MAC	IgM antibody capture
MB	Methylene blue
MNB	Magnetic nanobeads
MNP(s)	Magnetic nanoparticle(s)
mRNA	Messenger RNA
NALFIA	Nucleic acid lateral flow immuno assay
NASBA	Nucleic acid sequence-based amplification
NDV	Newcastle disease virus
NTA	Ni(ɪɪ)-nitrilotriacetic acid
ODN	Oligodinucleotide
pAb	Polyclonal antibody
PCR	Polymerase chain reaction
PEG	Poly(ethylene glycol)
pf HRP	*Plasmodium falciparum* histidine-rich protein
PFU	Plaque-forming unit
PIF	Powdered infant formulae
pLDH	*Plasmodium* lactate dehydrogenase
pNIPAm	Poly(*N*-isopropylacrylamide)
POC	Point of care
QD(s)	Quantum dot(s)
QR	Quick response
r-DNA/RNA	Recombinant DNA/RNA
RNALFIA	Ribonucleic acid LFIA
RT-LAMP	Reverse-transcription loop-mediated isothermal amplification
SEB	*Staphylococcus* enterotoxin B
SERS	Surface-enhanced raman scattering

SRB	Sulforhodamine B
ss	Single stranded
ss DNA	Single stranded DNA
TCID	Tissue culture infectious dose
UCP	Up-converting phosphor
VLP(s)	Virus-like particle(s)
WHO	World Health Organization
YFV	Yellow fever virus
ZIKV	Zika virus

Conflicts of interest

There are no conflicts to declare.

Acknowledgements

References

1 J. H. Leuvering, P. J. Thal, M. van der Waart and A. H. Schuurs, *J. Immunoassay*, 1980, **1**, 77–91.
2 E. C. Schramm, N. R. Staten, Z. Zhang, S. S. Bruce, C. Kellner, J. P. Atkinson, V. C. Kyttaris, G. C. Tsokos, M. Petri, E. Sander Connolly and P. K. Olson, *Anal. Biochem.*, 2015, **477**, 78–85.
3 N. De Giovanni and N. Fucci, *Curr. Med. Chem.*, 2013, **20**, 545–561.
4 R. Pacifici, M. Farre, S. Pichini, J. Ortuno, P. N. Roset, P. Zuccaro, J. Segura and R. de la Torre, *J. Anal. Toxicol.*, 2001, **25**, 144–146.
5 A. Carrio, C. Sampedro, J. L. Sanchez-Lopez, M. Pimienta and P. Campoy, *Sensors*, 2015, **15**, 29569–29593.
6 R. Kwizera, J. Nguna, A. Kiragga, J. Nakavuma, R. Rajasingham, D. R. Boulware and D. B. Meya, *PLoS One*, 2014, **9**, e103156.
7 S. Buhrer-Sekula, H. L. Smits, G. C. Gussenhoven, J. van Leeuwen, S. Amador, T. Fujiwara, P. R. Klatser and L. Oskam, *J. Clin. Microbiol.*, 2003, **41**, 1991–1995.
8 J. N. Jarvis, A. Percival, S. Bauman, J. Pelfrey, G. Meintjes, G. N. Williams, N. Longley, T. S. Harrison and T. R. Kozel, *Clin. Infect. Dis*, 2011, **53**, 1019–1023.
9 M. L. Moreno, A. Cebolla, A. Munoz-Suano, C. Carrillo-Carrion, I. Comino, A. Pizarro, F. Leon, A. Rodriguez-Herrera and C. Sousa, *Gut*, 2017, **66**, 250–257.
10 V. S. Vaidya, G. M. Ford, S. S. Waikar, Y. Wang, M. B. Clement, V. Ramirez, W. E. Glaab, S. P. Troth, F. D. Sistare, W. C. Prozialeck, J. R. Edwards, N. A. Bobadilla, S. C. Mefferd and J. V. Bonventre, *Kidney Int.*, 2009, **76**, 108–114.

11 S. H. Ang, M. Rambeli, T. M. Thevarajah, Y. B. Alias and S. M. Khor, *Biosens. Bioelectron.*, 2016, **78**, 187–193.
12 R. E. Biagini, D. L. Sammons, J. P. Smith, B. A. MacKenzie, C. A. Striley, J. E. Snawder, S. A. Robertson and C. P. Quinn, *Clin. Vaccine Immunol.*, 2006, **13**, 541–546.
13 S. Rosen, in *Lateral Flow Immunoassay*, ed. R. C. Wong and H. Y. Tse, Springer, New York, 2009, ch. 2, pp. 35–50.
14 X. Huang, Z. P. Aguilar, H. Xu, W. Lai and Y. Xiong, *Biosens. Bioelectron.*, 2016, **75**, 166–180.
15 K. M. Koczula and A. Gallotta, *Essays Biochem.*, 2016, **60**, 111–120.
16 World Health Organization, 2015, https://books.google.co.in/books?hl=en&lr=&id=Kl00DgAAQBAJ&oi=fnd&pg=PP1&dq=World+Health+Organization.+2015.+Mortality+and+global+health+estimates.+Geneva,+Switzerland:+World+Health+Organization&ots=8MrFnAPOwc&sig=2XZQEy7SlofM3888phKwJSe_dgc#v=onepage&q&f=false, Mortality and global health estimates. Geneva, Switzerland: World Health Organization, (accessed January 2018).
17 C. Dye, *Philos. Trans. R. Soc., B*, 2014, **369**, 20130426.
18 G. A. Posthuma-Trumpie, J. Korf and A. van Amerongen, *Anal. Bioanal. Chem.*, 2009, **393**, 569–582.
19 G. A. Posthuma-Trumpie, J. H. Wichers, M. Koets, L. B. Berendsen and A. van Amerongen, *Anal. Bioanal. Chem.*, 2012, **402**, 593–600.
20 Y. Xu, Y. Liu, Y. Wu, X. Xia, Y. Liao and Q. Li, *Anal. Chem.*, 2014, **86**, 5611–5614.
21 D. Quesada-Gonzalez and A. Merkoci, *Biosens. Bioelectron.*, 2015, **73**, 47–63.
22 E. B. Bahadır and M. K. Sezgintürk, *TrAC, Trends Anal. Chem.*, 2016, **82**, 286–306.
23 M. J. Raeisossadati, N. M. Danesh, F. Borna, M. Gholamzad, M. Ramezani, K. Abnous and S. M. Taghdisi, *Biosens. Bioelectron.*, 2016, **86**, 235–246.
24 K. Wang, W. Qin, Y. Hou, K. Xiao and W. Yan, *Nano Biomed. Eng.*, 2016, **8**, 172–183.
25 X. Gong, J. Cai, B. Zhang, Q. Zhao, J. Piao, W. Peng, W. Gao, D. Zhou, M. Zhao and J. Chang, *J. Mater. Chem. B*, 2017, **5**, 5079–5091.
26 M. Sajid, A.-N. Kawde and M. Daud, *J. Saudi Chem. Soc.*, 2015, **19**, 689–705.
27 B. Ngom, Y. Guo, X. Wang and D. Bi, *Anal. Bioanal. Chem.*, 2016, **408**, 3923.
28 J. Y. Lee, Y. A. Kim, M. Y. Kim, Y. T. Lee, B. D. Hammock and H. S. Lee, *Anal. Chim. Acta*, 2012, **757**, 69–74.
29 Rapid Lateral Flow Test Strips: Considerations for Product Development, Merck Millipore, Billerica https://www.emd-millipore.com/Web-US-Site/en_CA/-/USD/ShowDocument-Pronet?id=201306.12550 (accessed March, 2018).
30 I. H. Cho, S. M. Seo, E. H. Paek and S. H. Paek, *J. Chromatogr. B: Anal. Technol. Biomed. Life Sci.*, 2010, **878**, 271–277.
31 P. F. Mens, A. van Amerongen, P. Sawa, P. A. Kager and H. D. Schallig, *Diagn. Microbiol. Infect. Dis.*, 2008, **61**, 421–427.

32 Z. Wang, D. Zhi, Y. Zhao, H. Zhang, X. Wang, Y. Ru and H. Li, *Int. J. Nanomed.*, 2014, **9**, 1699–1707.

33 S. Takanashi, M. Okame, T. Shiota, M. Takagi, F. Yagyu, P. G. Tung, S. Nishimura, N. Katsumata, T. Igarashi, S. Okitsu and H. Ushijima, *J. Virol. Methods*, 2008, **148**, 1–8.

34 J. S. Ponti, in *Lateral Flow Immunoassay*, ed. R. C. Wong and H. Y. Tse, Springer, New York, 2009, ch. 2, pp. 35–50.

35 A. van Amerongen, D. van Loon, L. B. Berendsen and J. H. Wichers, *Clin. Chim. Acta*, 1994, **229**, 67–75.

36 J. A. Ho and M. R. Huang, *Anal. Chem.*, 2005, **77**, 3431–3436.

37 E. R. Goldman, A. R. Clapp, G. P. Anderson, H. T. Uyeda, J. M. Mauro, I. L. Medintz and H. Mattoussi, *Anal. Chem.*, 2004, **76**, 684–688.

38 P. Corstjens, M. Zuiderwijk, A. Brink, S. Li, H. Feindt, R. S. Niedbala and H. Tanke, *Clin. Chem.*, 2001, **47**, 1885–1893.

39 Y. C. Cao, R. Jin and C. A. Mirkin, *Science*, 2002, **297**, 1536–1540.

40 J. Hwang, S. Lee and J. Choo, *Nanoscale*, 2016, **8**, 11418–11425.

41 L. Blanco-Covian, V. Montes-Garcia, A. Girard, M. T. Fernandez-Abedul, J. Perez-Juste, I. Pastoriza-Santos, K. Faulds, D. Graham and M. C. Blanco-Lopez, *Nanoscale*, 2017, **9**, 2051–2058.

42 O. J. Clarke, B. L. Goodall, H. P. Hui, N. Vats and C. L. Brosseau, *Anal. Chem.*, 2017, **89**, 1405–1410.

43 M. Sanchez-Purra, M. Carre-Camps, H. de Puig, I. Bosch, L. Gehrke and K. Hamad-Schifferli, *ACS Infect. Dis.*, 2017, **3**, 767–776.

44 P. Sandström, M. Boncheva and B. Åkerman, *Langmuir*, 2003, **19**, 7537–7543.

45 J. M. de la Fuente and S. Penades, *Biochim. Biophys. Acta*, 2006, **1760**, 636–651.

46 S. Zeng, K.-T. Yong, I. Roy, X.-Q. Dinh, X. Yu and F. Luan, *Plasmonics*, 2011, **6**, 491.

47 A. K. Gupta and M. Gupta, *Biomaterials*, 2005, **26**, 3995–4021.

48 B. Pelaz, P. del Pino, P. Maffre, R. Hartmann, M. Gallego, S. Rivera-Fernandez, J. M. de la Fuente, G. U. Nienhaus and W. J. Parak, *ACS Nano*, 2015, **9**, 6996–7008.

49 A. K. Gupta, R. R. Naregalkar, V. D. Vaidya and M. Gupta, *Nanomedicine*, 2007, **2**, 23–39.

50 P. C. Soo, Y. T. Horng, P. R. Hsueh, B. J. Shen, J. Y. Wang, H. H. Tu, J. R. Wei, S. C. Hsieh, C. C. Huang and H. C. Lai, *J. Microbiol. Methods*, 2006, **66**, 440–448.

51 K. A. Edwards and A. J. Baeumner, *Anal. Bioanal. Chem.*, 2006, **386**, 1335–1343.

52 B. Y. Jung, S. C. Jung and C. H. Kweon, *J. Food Prot.*, 2005, **68**, 2140–2143.

53 J. Wang, W. N. Chen, K. X. Hu and W. Li, *Weisheng Yanjiu*, 2006, **35**, 439–441.

54 H. Qi, Z. Zhong, H. X. Zhou, C. Y. Deng, H. Zhu, J. F. Li, X. L. Wang and F. R. Li, *Int. J. Nanomed.*, 2011, **6**, 3033–3039.

55 Q. Y. Xie, Y. H. Wu, Q. R. Xiong, H. Y. Xu, Y. H. Xiong, K. Liu, Y. Jin and W. H. Lai, *Biosens. Bioelectron.*, 2014, **54**, 262–265.

56 J. Park, J. H. Shin and J. K. Park, *Anal. Chem.*, 2016, **88**, 3781–3788.

57 E. Morales-Narvaez, T. Naghdi, E. Zor and A. Merkoci, *Anal. Chem.*, 2015, **87**, 8573–8577.

58 K. H. Seo, P. S. Holt, H. D. Stone and R. K. Gast, *Int. J. Food Microbiol.*, 2003, **87**, 139–144.

59 Z. Fang, W. Wu, X. Lu and L. Zeng, *Biosens. Bioelectron.*, 2014, **56**, 192–197.

60 C.-C. Liu, C.-Y. Yeung, P.-H. Chen, M.-K. Yeh and S.-Y. Hou, *Food Chem.*, 2013, **141**, 2526–2532.

61 S. Rong-Hwa, T. Shiao-Shek, C. Der-Jiang and H. Yao-Wen, *Food Chem.*, 2010, **118**, 462–466.

62 M. Fisher, Y. Atiya-Nasagi, I. Simon, M. Gordin, A. Mechaly and S. Yitzhaki, *Lett. Appl. Microbiol.*, 2009, **48**, 413–418.

63 D. B. Wang, B. Tian, Z. P. Zhang, J. Y. Deng, Z. Q. Cui, R. F. Yang, X. Y. Wang, H. P. Wei and X. E. Zhang, *Biosens. Bioelectron.*, 2013, **42**, 661–667.

64 D. B. Wang, B. Tian, Z. P. Zhang, X. Y. Wang, J. Fleming, L. J. Bi, R. F. Yang and X. E. Zhang, *Biosens. Bioelectron.*, 2015, **67**, 608–614.

65 N. Nakasone, C. Toma, Y. Lu and M. Iwanaga, *Diagn. Microbiol. Infect. Dis.*, 2007, **57**, 21–25.

66 K. Kawatsu, Y. Kumeda, M. Taguchi, W. Yamazaki-Matsune, M. Kanki and K. Inoue, *J. Clin. Microbiol.*, 2008, **46**, 1226–1231.

67 L. Yu, P. Li, X. Ding and Q. Zhang, *Talanta*, 2017, **165**, 167–175.

68 D. Tang, J. C. Sauceda, Z. Lin, S. Ott, E. Basova, I. Goryacheva, S. Biselli, J. Lin, R. Niessner and D. Knopp, *Biosens. Bioelectron.*, 2009, **25**, 514–518.

69 Y.-M. Huang, D.-F. Liu, W.-H. Lai, Y.-H. Xiong, W.-C. Yang, K. Liu and S.-Y. Wang, *Chin. J. Anal. Chem.*, 2014, **42**, 654–659.

70 D. Liu, Y. Huang, S. Wang, K. Liu, M. Chen, Y. Xiong, W. Yang and W. Lai, *Food Control*, 2015, **51**, 218–224.

71 L. Anfossi, F. Di Nardo, S. Cavalera, C. Giovannoli, G. Spano, E. S. Speranskaya, I. Y. Goryacheva and C. Baggiani, *Microchim. Acta*, 2018, **185**, 94.

72 T. Klewitz, F. Gessler, H. Beer, K. Pflanz and T. Scheper, *Sens. Actuators, B*, 2006, **113**, 582–589.

73 D. J. Chiao, J. J. Wey, R. H. Shyu and S. S. Tang, *Hybridoma*, 2008, **27**, 31–35.

74 K. H. Ching, A. Lin, J. A. McGarvey, L. H. Stanker and R. Hnasko, *J. Immunol. Methods*, 2012, **380**, 23–29.

75 S.-H. Huang, H.-C. Wei and Y.-C. Lee, *Food Control*, 2007, **18**, 893–897.

76 S.-H. Huang, *Sens. Actuators, B*, 2007, **127**, 335–340.

77 S. Wiriyachaiporn, P. H. Howarth, K. D. Bruce and L. A. Dailey, *Diagn. Microbiol. Infect. Dis.*, 2013, **75**, 28–36.

78 N. Khreich, P. Lamourette, H. Boutal, K. Devilliers, C. Creminon and H. Volland, *Anal. Biochem.*, 2008, **377**, 182–188.

79 Y. Ju, H. J. Hao, G. H. Xiong, H. R. Geng, Y. L. Zheng, J. Wang, Y. Cao, Y. H. Yang, X. H. Cai and Y. Q. Jiang, *Vet. Immunol. Immunopathol.*, 2010, **133**, 207–211.

80 T. Nakayama, J. Zhao, D. Takeuchi, A. Kerdsin, P. Chiranairadul, P. Areeratana, P. Loetthong, A. Pienpringam, Y. Akeda and K. Oishi, *Biosens. Bioelectron.*, 2014, **60**, 175–179.

81 X. Zhang, J. Zhou, C. Zhang, D. Zhang and X. Su, *RSC Adv.*, 2016, **6**, 1279–1287.

82 M. Blazkova, B. Javurkova, L. Fukal and P. Rauch, *Biosens. Bioelectron.*, 2011, **26**, 2828–2834.

83 H. L. Smits, C. K. Eapen, S. Sugathan, M. Kuriakose, M. H. Gasem, C. Yersin, D. Sasaki, B. Pujianto, M. Vestering, T. H. Abdoel and G. C. Gussenhoven, *Clin. Diagn. Lab. Immunol.*, 2001, **8**, 166–169.

84 A. B. Nurul Najian, E. A. Engku Nur Syafirah, N. Ismail, M. Mohamed and C. Y. Yean, *Anal. Chim. Acta*, 2016, **903**, 142–148.

85 C. Y. Yu, G. Y. Ang, A. L. Chua, E. H. Tan, S. Y. Lee, G. Falero-Diaz, O. Otero, I. Rodriguez, F. Reyes, A. Acosta, M. E. Sarmiento, S. Ghosh, T. Ramamurthy, C. Yean Yean, P. Lalitha and M. Ravichandran, *J. Microbiol. Methods*, 2011, **86**, 277–282.

86 C. Pengsuk, P. Chaivisuthangkura, S. Longyant and P. Sithigorngul, *Biosens. Bioelectron.*, 2013, **42**, 229–235.

87 L. Wang, J. Zhang, H. Bai, X. Li, P. Lv and A. Guo, *Appl. Biochem. Biotechnol.*, 2014, **173**, 1073–1082.

88 A. J. Herring, R. C. Ballard, V. Pope, R. A. Adegbola, J. Changalucha, D. W. Fitzgerald, E. W. Hook, A. Kubanova, S. Mananwatte, J. W. Pape, A. W. Sturm, B. West, Y. P. Yin and R. W. Peeling, *Sex. Transm. Infect.*, 2006, **82**, v7–v12.

89 P. Mdluli, P. Tetyana, N. Sosibo, H. van der Walt, M. Mlambo, A. Skepu and R. Tshikhudo, *Biosens. Bioelectron.*, 2014, **54**, 1–6.

90 H. Liu, F. Zhan, F. Liu, M. Zhu, X. Zhou and D. Xing, *Biosens. Bioelectron.*, 2014, **62**, 38–46.

91 M. Blažková, M. Koets, P. Rauch and A. van Amerongen, *Eur. Food Res. Technol.*, 2009, **229**, 867.

92 Z. Lin, S. Cheng, Q. Yan, X. Liu, W. Zheng, X. Hu, J. Li, J. Zhang, T. Xiang, J. Zheng and J. Zhang, *Clin. Biochem.*, 2015, **48**, 1298–1303.

93 F. Chen, X. Ming, X. Chen, M. Gan, B. Wang, F. Xu and H. Wei, *Biosens. Bioelectron.*, 2014, **61**, 306–313.

94 J. A. Ho, S. C. Zeng, W. H. Tseng, Y. J. Lin and C. H. Chen, *Anal. Bioanal. Chem.*, 2008, **391**, 479–485.

95 S. Xia, Z. Yu, D. Liu, C. Xu and W. Lai, *Food Control*, 2016, **59**, 507–512.

96 Q. Qu, Z. Zhu, Y. Wang, Z. Zhong, J. Zhao, F. Qiao, X. Du, Z. Wang, R. Yang, L. Huang, Y. Yu, L. Zhou and Z. Chen, *J. Microbiol. Methods*, 2009, **79**, 121–123.

97 F. Zhang, M. Zou, Y. Chen, J. Li, Y. Wang, X. Qi and Q. Xue, *Biosens. Bioelectron.*, 2014, **51**, 29–35.

98 Z. Liang, X. Wang, W. Zhu, P. Zhang, Y. Yang, C. Sun, J. Zhang, X. Wang, Z. Xu, Y. Zhao, R. Yang, S. Zhao and L. Zhou, *ACS Appl. Mater. Interfaces*, 2017, **9**, 3497–3504.

99 C. Z. Li, K. Vandenberg, S. Prabhulkar, X. Zhu, L. Schneper, K. Methee, C. J. Rosser and E. Almeide, *Biosens. Bioelectron.*, 2011, **26**, 4342–4348.

100 J. H. Shin, J. Hong, H. Go, J. Park, M. Kong, S. Ryu, K. P. Kim, E. Roh and J. K. Park, *J. Agric. Food Chem.*, 2018, **66**, 290–297.

101 S. Shafazand, R. Doyle, S. Ruoss, A. Weinacker and T. A. Raffin, *Chest*, 1999, **116**, 1369–1376.

102 Z. A. Kanafani, A. Ghossain, A. I. Sharara, J. M. Hatem and S. S. Kanj, *Emerging Infect. Dis.*, 2003, **9**, 520–525.

103 L. W. Riley, R. S. Remis, S. D. Helgerson, H. B. McGee, J. G. Wells, B. R. Davis, R. J. Hebert, E. S. Olcott, L. M. Johnson, N. T. Hargrett, P. A. Blake and M. L. Cohen, *N. Engl. J. Med.*, 1983, **308**, 681–685.

104 W. Wu, S. Zhao, Y. Mao, Z. Fang, X. Lu and L. Zeng, *Anal. Chim. Acta*, 2015, **861**, 62–68.

105 C. Pohlmann, I. Dieser and M. Sprinzl, *Analyst*, 2014, **139**, 1063–1071.

106 R. V. Tauxe, C. M. Patton, P. Edmonds, T. J. Barrett, D. J. Brenner and P. A. Blake, *J. Clin. Microbiol.*, 1985, **21**, 222–225.

107 J. Singh, S. Sharma and S. Nara, *Food Chem.*, 2015, **170**, 470–483.

108 H. D. Shukla and S. K. Sharma, *Crit. Rev. Microbiol.*, 2005, **31**, 11–18.

109 S. S. Arnon, R. Schechter, T. V. Inglesby, D. A. Henderson, J. G. Bartlett, M. S. Ascher, E. Eitzen, A. D. Fine, J. Hauer, M. Layton, S. Lillibridge, M. T. Osterholm, T. O'Toole, G. Parker, T. M. Perl, P. K. Russell, D. L. Swerdlow, K. Tonat and B. Working Group on Civilian, *J. Am. Med. Assoc.*, 2001, **285**, 1059–1070.

110 J. Kadariya, T. C. Smith and D. Thapaliya, *BioMed Res. Int.*, 2014, **2014**, 827965.

111 M. C. Heidt, W. Mohamed, T. Hain, P. R. Vogt, T. Chakraborty and E. Domann, *J. Clin. Microbiol.*, 2005, **43**, 4898–4901.

112 S. Sriskandan and J. D. Slater, *PLoS Med.*, 2006, **3**, e187.

113 X. Jiang, Y. Ni, Y. Jiang, F. Yuan, L. Han, M. Li, H. Liu, L. Yang and Y. Lu, *J. Clin. Microbiol.*, 2005, **43**, 826–831.

114 M. L. Mezzatesta, F. Gona and S. Stefani, *Future Microbiol.*, 2012, **7**, 887–902.

115 R. Chauhan, J. Singh, T. Sachdev, T. Basu and B. D. Malhotra, *Biosens. Bioelectron.*, 2016, **81**, 532–545.

116 S. Shan, W. Lai, Y. Xiong, H. Wei and H. Xu, *J. Agric. Food Chem.*, 2015, **63**, 745–753.

117 A.-L. Välimaa, A. Tilsala-Timisjärvi and E. Virtanen, *Food Control*, 2015, **55**, 103–114.

118 X. Wang, R. Niessner, D. Tang and D. Knopp, *Anal. Chim. Acta*, 2016, **912**, 10–23.

119 T. Yang, H. Huang, F. Zhu, Q. Lin, L. Zhang and J. Liu, *Sensors*, 2016, **16**, 1118.

120 A. Ratsimbasoa, A. Randriamanantena, R. Raherinjafy, N. Rasoarilalao and D. Menard, *Am. J. Trop. Med. Hyg.*, 2007, **76**, 481–485.

121 J. D. Swartz, C. P. Gulka, F. R. Haselton and D. W. Wright, *Langmuir*, 2011, **27**, 15330–15339.

122 M. A. Nash, J. N. Waitumbi, A. S. Hoffman, P. Yager and P. S. Stayton, *ACS Nano*, 2012, **6**, 6776–6785.

123 C. L. Mthembu, M. I. Sabela, M. Mlambo, L. M. Madikizela, S. Kanchi, H. Gumede and P. S. Mdluli, *Anal. Methods*, 2017, **9**, 5943–5951.

124 D. Y. Pereira, R. Y. Chiu, S. C. Zhang, B. M. Wu and D. T. Kamei, *Anal. Chim. Acta*, 2015, **882**, 83–89.

125 L. Rivas, A. de la Escosura-Muñiz, L. Serrano, L. Altet, O. Francino, A. Sánchez and A. Merkoçi, *Nano Res.*, 2015, **8**, 3704–3714.

126 P. L. Corstjens, L. van Lieshout, M. Zuiderwijk, D. Kornelis, H. J. Tanke, A. M. Deelder and G. J. van Dam, *J. Clin. Microbiol.*, 2008, **46**, 171–176.

127 G. J. van Dam, C. J. de Dood, M. Lewis, A. M. Deelder, L. van Lieshout, H. J. Tanke, L. H. van Rooyen and P. L. Corstjens, *Exp. Parasitol.*, 2013, **135**, 274–282.

128 F. Peng, Z. Wang, S. Zhang, R. Wu, S. Hu, Z. Li, X. Wang and D. Bi, *Clin. Vaccine Immunol.*, 2008, **15**, 569–574.

129 V. Veguilla, K. Hancock, J. Schiffer, P. Gargiullo, X. Lu, D. Aranio, A. Branch, L. Dong, C. Holiday, F. Liu, E. Steward-Clark, H. Sun, B. Tsang, D. Wang, M. Whaley, Y. Bai, L. Cronin, P. Browning, H. Dababneh, H. Noland, L. Thomas, L. Foster, C. P. Quinn, S. D. Soroka and J. M. Katz, *J. Clin. Microbiol.*, 2011, **49**, 2210–2215.

130 Y. T. Kim, J. H. Jung, Y. K. Choi and T. S. Seo, *Biosens. Bioelectron.*, 2014, **61**, 485–490.

131 J. H. Jung, S. J. Oh, Y. T. Kim, S. Y. Kim, W. J. Kim, J. Jung and T. S. Seo, *Anal. Chim. Acta*, 2015, **853**, 541–547.

132 K. Mitamura, H. Shimizu, M. Yamazaki, M. Ichikawa, K. Nagai, J. Katada, A. Wada, C. Kawakami and N. Sugaya, *J. Virol. Methods*, 2013, **194**, 123–128.

133 N. Wiriyachaiporn, W. Maneeprakorn, C. Apiwat and T. Dharakul, *Microchim. Acta*, 2015, **182**, 85–93.

134 T. T. Le, P. Chang, D. J. Benton, J. W. McCauley, M. Iqbal and A. E. G. Cass, *Anal. Chem.*, 2017, **89**, 6781–6786.

135 S. Bamrungsap, C. Apiwat, W. Chantima, T. Dharakul and N. Wiriyachaiporn, *Microchim. Acta*, 2014, **181**, 223–230.

136 D. T. Lau, H. Ma, S. M. Lemon, E. Doo, M. G. Ghany, E. Miskovsky, G. L. Woods, Y. Park and J. H. Hoofnagle, *J. Viral Hepatitis*, 2003, **10**, 331–334.

137 K. S. Myint, M. Guan, H. Y. Chen, Y. Lu, D. Anderson, T. Howard, H. Noedl and M. P. Mammen Jr., *Am. J. Trop. Med. Hyg.*, 2005, **73**, 942–946.

138 H. Y. Chen, Y. Lu, T. Howard, D. Anderson, P. Y. Fong, W. P. Hu, C. P. Chia and M. Guan, *Clin. Diagn. Lab. Immunol.*, 2005, **12**, 593–598.

139 T. Salminen, E. Juntunen, N. Khanna, K. Pettersson and S. M. Talha, *J. Virol. Methods*, 2016, **228**, 67–73.

140 L. Li, L. Zhou, Y. Yu, Z. Zhu, C. Lin, C. Lu and R. Yang, *Diagn. Microbiol. Infect. Dis.*, 2009, **63**, 165–172.

141 S. Huaibin, Y. Hang, N. Jin Zhong, X. Shasha, Z. Changhua, M. Lan and L. Lin Song, *Nanotechnology*, 2011, **22**, 375602.

142 J. Shen, Y. Zhou, F. Fu, H. Xu, J. Lv, Y. Xiong and A. Wang, *Talanta*, 2015, **142**, 145–149.

143 US Food and Drug Administration, https://www.fda.gov/downloads/biologicsbloodvaccines/bloodbloodproducts/approvedproducts/premarketapprovalspmas/ucm364698.pdf, (accessed January 2018).

144 S. Workman, S. K. Wells, C. P. Pau, S. M. Owen, X. F. Dong, R. LaBorde and T. C. Granade, *J. Virol. Methods*, 2009, **160**, 14–21.

145 H. H. Lee, M. A. Dineva, Y. L. Chua, A. V. Ritchie, I. Ushiro-Lumb and C. A. Wisniewski, *J. Infect. Dis.*, 2010, **201**(Suppl 1), S65–S72.

146 B. A. Rohrman, V. Leautaud, E. Molyneux and R. R. Richards-Kortum, *PLoS One*, 2012, **7**, e45611.

147 Z. A. Parpia, R. Elghanian, A. Nabatiyan, D. R. Hardie and D. M. Kelso, *JAIDS, J. Acquired Immune Defic. Syndr.*, 2010, **55**, 413–419.

148 C. N. Loynachan, M. R. Thomas, E. R. Gray, D. A. Richards, J. Kim, B. S. Miller, J. C. Brookes, S. Agarwal, V. Chudasama, R. A. McKendry and M. M. Stevens, *ACS Nano*, 2018, **12**, 279–288.

149 J. Hu, L. Wang, F. Li, Y. L. Han, M. Lin, T. J. Lu and F. Xu, *Lab Chip*, 2013, **13**, 4352–4357.

150 X. Fu, Z. Cheng, J. Yu, P. Choo, L. Chen and J. Choo, *Biosens. Bioelectron.*, 2016, **78**, 530–537.

151 H. Tsutsumi, K. Ouchi, M. Ohsaki, T. Yamanaka, Y. Kuniya, Y. Takeuchi, C. Nakai, H. Meguro and S. Chiba, *J. Clin. Microbiol.*, 1999, **37**, 2007–2009.

152 A. Wada, Y. Sakoda, T. Oyamada and H. Kida, *J. Virol. Methods*, 2011, **178**, 82–86.

153 X. Li, D. Lu, Z. Sheng, K. Chen, X. Guo, M. Jin and H. Han, *Talanta*, 2012, **100**, 1–6.

154 N. A. Shaikh, J. Ge, Y. X. Zhao, P. Walker and M. Drebot, *Clin. Chem.*, 2007, **53**, 2031–2034.

155 A. R. Sambol and S. H. Hinrichs, *J. Virol. Methods*, 2009, **157**, 223–226.

156 S. D. Blacksell, J. A. Doust, P. N. Newton, S. J. Peacock, N. P. Day and A. M. Dondorp, *Trans. R. Soc. Trop. Med. Hyg.*, 2006, **100**, 775–784.

157 S. D. Blacksell, P. N. Newton, D. Bell, J. Kelley, M. P. Mammen Jr., D. W. Vaughn, V. Wuthiekanun, A. Sungkakum, A. Nisalak and N. P. Day, *Clin. Infect. Dis*, 2006, **42**, 1127–1134.

158 T. T. Nga, K. T. Thai, H. L. Phuong, P. T. Giao, Q. Hung le, T. Q. Binh, V. T. Mai, N. Van Nam and P. J. de Vries, *Clin. Vaccine Immunol.*, 2007, **14**, 799–801.

159 P. Dussart, L. Petit, B. Labeau, L. Bremand, A. Leduc, D. Moua, S. Matheus and L. Baril, *PLoS Neglected Trop. Dis.*, 2008, **2**, e280.

160 M. Moorthy, S. Chandy, K. Selvaraj and A. M. Abraham, *Indian J. Med. Microbiol.*, 2009, **27**, 254–256.

161 R. Lima Mda, R. M. Nogueira, H. G. Schatzmayr and F. B. dos Santos, *PLoS Neglected Trop. Dis.*, 2010, **4**, e738.

162 L. Osorio, M. Ramirez, A. Bonelo, L. A. Villar and B. Parra, *Virol. J.*, 2010, **7**, 361.

163 V. Tricou, H. T. Vu, N. V. Quynh, C. V. Nguyen, H. T. Tran, J. Farrar, B. Wills and C. P. Simmons, *BMC Infect. Dis.*, 2010, **10**, 142.

164 Y. Zhang, J. Bai and J. Y. Ying, *Lab Chip*, 2015, **15**, 1465–1471.

165 MD Doctors Direct, http://www.mddoctorsdirect.com/sites/default/files/product-pdf/46FK10_Chikungunya-IgM(D)_CE(Rev.4).pdf, (accessed January 2018).

166 CTKbiotech Online, http://ctkbiotech.com/ctk-product/chikungunya-igm-combo-rapid-test-ce/, (accessed January 2018).

167 S. D. Blacksell, A. Tanganuchitcharnchai, R. G. Jarman, R. V. Gibbons, D. H. Paris, M. S. Bailey, N. P. Day, R. Premaratna, D. G. Lalloo and H. J. de Silva, *Clin. Vaccine Immunol.*, 2011, **18**, 1773–1775.

168 H. Kosasih, S. Widjaja, E. Surya, S. H. Hadiwijaya, D. P. Butarbutar, U. A. Jaya, Nurhayati, B. Alisjahbana and M. Williams, *Southeast Asian J. Trop. Med. Public Health*, 2012, **43**, 55–61.

169 C. M. Prat, O. Flusin, A. Panella, B. Tenebray, R. Lanciotti and I. Leparc-Goffart, *Emerging Infect. Dis.*, 2014, **20**, 2129–2132.

170 E. I. Laderman, E. Whitworth, E. Dumaual, M. Jones, A. Hudak, W. Hogrefe, J. Carney and J. Groen, *Clin. Vaccine Immunol.*, 2008, **15**, 159–163.

171 J. Li, M. Zou, Y. Chen, Q. Xue, F. Zhang, B. Li, Y. Wang, X. Qi and Y. Yang, *Anal. Chim. Acta*, 2013, **782**, 54–58.

172 P. Brangel, A. Sobarzo, C. Parolo, B. S. Miller, P. D. Howes, S. Gelkop, J. J. Lutwama, J. M. Dye, R. A. McKendry, L. Lobel and M. M. Stevens, *ACS Nano*, 2018, **12**, 63–73.

173 D. Duan, K. Fan, D. Zhang, S. Tan, M. Liang, Y. Liu, J. Zhang, P. Zhang, W. Liu, X. Qiu, G. P. Kobinger, G. F. Gao and X. Yan, *Biosens. Bioelectron.*, 2015, **74**, 134–141.

174 A. E. Hagstrom, G. Garvey, A. S. Paterson, S. Dhamane, M. Adhikari, M. K. Estes, U. Strych, K. Kourentzi, R. L. Atmar and R. C. Willson, *PLoS One*, 2015, **10**, e0126571.

175 I. Bosch, H. de Puig, M. Hiley, M. Carre-Camps, F. Perdomo-Celis, C. F. Narvaez, D. M. Salgado, D. Senthoor, M. O'Grady, E. Phillips, A. Durbin, D. Fandos, H. Miyazaki, C. W. Yen, M. Gelvez-Ramirez, R. V. Warke, L. S. Ribeiro, M. M. Teixeira, R. P. Almeida, J. E. Munoz-Medina, J. E. Ludert, M. L. Nogueira, T. E. Colombo, A. C. B. Terzian, P. T. Bozza, A. S. Calheiros, Y. R. Vieira, G. Barbosa-Lima, A. Vizzoni, J. Cerbino-Neto, F. A. Bozza, T. M. L. Souza, M. R. O. Trugilho, A. M. B. de Filippis, P. C. de Sequeira, E. T. A. Marques, T. Magalhaes, F. J. Diaz, B. N. Restrepo, K. Marin, S. Mattar, D. Olson, E. J. Asturias, M. Lucera, M. Singla, G. R. Medigeshi, N. de Bosch, J. Tam, J. Gomez-Marquez, C. Clavet, L. Villar, K. Hamad-Schifferli and L. Gehrke, *Sci. Transl. Med.*, 2017, **9**, eaan1589.

176 J. H. Lee, H. S. Seo, J. H. Kwon, H. T. Kim, K. C. Kwon, S. J. Sim, Y. J. Cha and J. Lee, *Biosens. Bioelectron.*, 2015, **69**, 213–225.

177 C. W. Yen, H. de Puig, J. O. Tam, J. Gomez-Marquez, I. Bosch, K. Hamad-Schifferli and L. Gehrke, *Lab Chip*, 2015, **15**, 1638–1641.

178 X. Wang, N. Choi, Z. Cheng, J. Ko, L. Chen and J. Choo, *Anal. Chem.*, 2017, **89**, 1163–1169.

179 S. Kersting, V. Rausch, F. F. Bier and M. von Nickisch-Rosenegk, *Malar. J*, 2014, **13**, 99.

180 M. S. Cordray and R. R. Richards-Kortum, *Am. J. Trop. Med. Hyg.*, 2012, **87**, 223–230.

181 A. H. Moody and P. L. Chiodini, *Br. J. Biomed. Sci.*, 2002, **59**, 228–231.

182 S. Knecht, D. Ricklin, A. N. Eberle and B. Ernst, *J. Mol. Recognit.*, 2009, **22**, 270–279.

183 B. Gryseels, K. Polman, J. Clerinx and L. Kestens, *Lancet*, 2006, **368**, 1106–1118.

184 S. Cui and G. Tong, *J. Vet. Diagn. Invest.*, 2008, **20**, 567–571.

185 D. Peng, S. Hu, Y. Hua, Y. Xiao, Z. Li, X. Wang and D. Bi, *Vet. Immunol. Immunopathol.*, 2007, **117**, 17–25.

186 D. H. Whang and T. Um, *Korean J. Lab. Med.*, 2005, **25**, 186–191.

187 Y. Khudyakov and S. Kamili, *Virus Res.*, 2011, **161**, 84–92.

188 M. H. K. Ansari, M. D. Omrani and V. Movahedi, *Hepatitis Mon.*, 2007, **7**, 87–91.

189 P. Yager, E. Fu, T. Liang, B. Lutz and J. L. Osborn, 15th International Conference on Miniaturized Systems for Chemistry and Life Sciences 2011, MicroTAS 2011, vol. 3, pp. 2092–2095.

190 G. Rezza, L. Nicoletti, R. Angelini, R. Romi, A. C. Finarelli, M. Panning, P. Cordioli, C. Fortuna, S. Boros, F. Magurano, G. Silvi, P. Angelini, M. Dottori, M. G. Ciufolini, G. C. Majori, A. Cassone and C. s. group, *Lancet*, 2007, **370**, 1840–1846.

191 F. Staikowsky, F. Talarmin, P. Grivard, A. Souab, I. Schuffenecker, K. Le Roux, M. Lecuit and A. Michault, *PLoS One*, 2009, **4**, e7603.

192 W. Van Bortel, F. Dorleans, J. Rosine, A. Blateau, D. Rousset, S. Matheus, I. Leparc-Goffart, O. Flusin, C. Prat, R. Cesaire, F. Najioullah, V. Ardillon, E. Balleydier, L. Carvalho, A. Lemaitre, H. Noel, V. Servas, C. Six, M. Zurbaran, L. Leon, A. Guinard, J. van den Kerkhof, M. Henry, E. Fanoy, M. Braks, J. Reimerink, C. Swaan, R. Georges, L. Brooks, J. Freedman, B. Sudre and H. Zeller, *Euro. Surveill.*, 2014, **19**, 20759.

193 E. Burdino, G. Calleri, P. Caramello and V. Ghisetti, *Emerging Infect. Dis.*, 2016, **22**, 1837–1839.

194 Centers for Disease Control and Prevention, https://www.cdc.gov/vhf/ebola/outbreaks/history/chronology.html (accessed January 2018).

195 W. H. O. Ebola Response Team, B. Aylward, P. Barboza, L. Bawo, E. Bertherat, P. Bilivogui, I. Blake, R. Brennan, S. Briand, J. M. Chakauya, K. Chitala, R. M. Conteh, A. Cori, A. Croisier, J. M. Dangou, B. Diallo, C. A. Donnelly, C. Dye, T. Eckmanns, N. M. Ferguson, P. Formenty, C. Fuhrer, K. Fukuda, T. Garske, A. Gasasira, S. Gbanyan, P. Graaff, E. Heleze, A. Jambai, T. Jombart, F. Kasolo, A. M. Kadiobo, S. Keita, D. Kertesz, M. Kone, C. Lane, J. Markoff, M. Massaquoi, H. Mills, J. M. Mulba, E. Musa, J. Myhre, A. Nasidi, E. Nilles, P. Nouvellet,

D. Nshimirimana, I. Nuttall, T. Nyenswah, O. Olu, S. Pendergast, W. Perea, J. Polonsky, S. Riley, O. Ronveaux, K. Sakoba, R. Santhana Gopala Krishnan, M. Senga, F. Shuaib, M. D. Van Kerkhove, R. Vaz, N. Wijekoon Kannangarage and Z. Yoti, *N. Engl. J. Med.*, 2014, **371**, 1481–1495.

196 H. Bourhy, P. E. Rollin, J. Vincent and P. Sureau, *J. Clin. Microbiol.*, 1989, **27**, 519–523.

197 A. Nishizono, P. Khawplod, K. Ahmed, K. Goto, S. Shiota, K. Mifune, T. Yasui, K. Takayama, Y. Kobayashi, K. Mannen, V. Tepsumethanon, C. Mitmoonpitak, S. Inoue and K. Morimoto, *Microbiol. Immunol.*, 2008, **52**, 243–249.

198 B. Kang, J. Oh, C. Lee, B. K. Park, Y. Park, K. Hong, K. Lee, B. Cho and D. Song, *J. Virol. Methods*, 2007, **145**, 30–36.

199 S. Kasempimolporn, W. Saengseesom, S. Huadsakul, S. Boonchang and V. Sitprija, *J. Vet. Diagn. Invest.*, 2011, **23**, 1197–1201.

200 D. K. Yang, E. K. Shin, Y. I. Oh, K. W. Lee, C. S. Lee, S. Y. Kim, J. A. Lee and J. Y. Song, *J. Vet. Sci.*, 2012, **13**, 43–48.

201 P. Sharma, C. K. Singh and D. Narang, *Vet. World*, 2015, **8**, 135–138.

202 World Health Organization, http://www.who.int/hiv/topics/vct/about/en/ (accessed January, 2018).

203 G. Wu and M. H. Zaman, *Bull. W. H. O.*, 2012, **90**, 914–920.

204 H. Arai, B. Petchclai, K. Khupulsup, T. Kurimura and K. Takeda, *J. Clin. Microbiol.*, 1999, **37**, 367–370.

205 S. Aidoo, W. K. Ampofo, J. A. Brandful, S. V. Nuvor, J. K. Ansah, N. Nii-Trebi, J. S. Barnor, F. Apeagyei, T. Sata, D. Ofori-Adjei and K. Ishikawa, *J. Clin. Microbiol.*, 2001, **39**, 2572–2575.

206 R. Ribeiro-Rodrigues, L. Ferreira da Silva Pinto Neto, C. B. Cunha, V. P. Cabral and R. Dietze, *Clin. Diagn. Lab. Immunol.*, 2003, **10**, 303–307.

207 T. C. Granade, B. S. Parekh, P. M. Tih, T. Welty, E. Welty, M. Bulterys, G. Ndikintum, G. Nkuoh and S. Tancho, *Clin. Diagn. Lab. Immunol.*, 2005, **12**, 855–860.

208 Centers for Disease Control and Prevention, https://hiv-tests-advantages-disadvantages.pdf (accessed January, 2018).

209 S. Phillips, T. C. Granade, C. P. Pau, D. Candal, D. J. Hu and B. S. Parekh, *Clin. Diagn. Lab. Immunol.*, 2000, **7**, 698–699.

210 F. Ketema, C. Zeh, D. C. Edelman, R. Saville and N. T. Constantine, *J. Acquired Immune Defic. Syndr.*, 2001, **27**, 63–70.

211 H. Syed Iqbal, P. Balakrishnan, K. G. Murugavel and S. Suniti, *J. Clin. Lab. Anal.*, 2008, **22**, 178–185.

212 Y. Wang, H. Xu, M. Wei, H. Gu, Q. Xu and W. Zhu, *Mater. Sci. Eng., C*, 2009, **29**, 714–718.

213 T. C. Granade, S. Workman, S. K. Wells, A. N. Holder, S. M. Owen and C. P. Pau, *Clin. Vaccine Immunol.*, 2010, **17**, 1034–1039.

214 M. D. Lindsley, N. Mekha, H. C. Baggett, Y. Surinthong, R. Autthateinchai, P. Sawatwong, J. R. Harris, B. J. Park, T. Chiller, S. A. Balajee and N. Poonwan, *Clin. Infect. Dis*, 2011, **53**, 321–325.

215 E. Uchio, K. Aoki, W. Saitoh, N. Itoh and S. Ohno, *Ophthalmology*, 1997, **104**, 1294–1299.

216 T. Fujimoto, T. Okafuji, T. Okafuji, M. Ito, S. Nukuzuma, M. Chikahira and O. Nishio, *J. Clin. Microbiol.*, 2004, **42**, 5489–5492.

217 G. L. Campbell, A. A. Marfin, R. S. Lanciotti and D. J. Gubler, *Lancet Infect. Dis.*, 2002, **2**, 519–529.

218 K. A. Gyure, *J. Neuropathol. Exp. Neurol.*, 2009, **68**, 1053–1060.

219 P. Koraka, H. Zeller, M. Niedrig, A. D. Osterhaus and J. Groen, *Microbes Infect.*, 2002, **4**, 1209–1215.

220 A. K. Malan, P. J. Stipanovich, T. B. Martins, H. R. Hill and C. M. Litwin, *Am. J. Clin. Pathol.*, 2003, **119**, 508–515.

221 A. K. Malan, T. B. Martins, H. R. Hill and C. M. Litwin, *J. Clin. Microbiol.*, 2004, **42**, 727–733.

222 G. E. Fridley, H. Le and P. Yager, *Anal. Chem.*, 2014, **86**, 6447–6453.

223 J. Hu, S. Wang, L. Wang, F. Li, B. Pingguan-Murphy, T. J. Lu and F. Xu, *Biosens. Bioelectron.*, 2014, **54**, 585–597.

224 V. Venkatraman and A. J. Steckl, *Biosens. Bioelectron.*, 2015, **74**, 150–155.

225 J. Li and J. Macdonald, *Biosens. Bioelectron.*, 2016, **85**, 998–999.

226 X. Cao, Y. Ye and S. Liu, *Anal. Biochem.*, 2011, **417**, 1–16.